

# BiMa: Towards Biases Mitigation for Text-Video Retrieval via Scene Element Guidance

Huy Le<sup>1</sup>   Nhat Chung<sup>1</sup>   Tung Kieu<sup>2,3</sup>   Anh Nguyen<sup>4</sup>   Ngan Le<sup>5</sup>

<sup>1</sup>FPT Software AI Center, Vietnam   <sup>2</sup>Aalborg University, Denmark   <sup>3</sup>Pioneer Centre for AI, Denmark

<sup>4</sup>University of Liverpool, UK   <sup>5</sup>AICV Lab, University of Arkansas, USA

{huylda1, nhaticm3}@fpt.com   tungkvt@cs.aau.dk   anh.nguyen@liverpool.ac.uk   thile@uark.edu

## Abstract

Text-video retrieval (TVR) systems often suffer from visual-linguistic biases present in datasets, which cause pre-trained vision-language models to overlook key details. To address this, we propose BiMa, a novel framework designed to mitigate biases in both visual and textual representations. Our approach begins by generating scene elements that characterize each video by identifying relevant entities/objects and activities. For visual debiasing, we integrate these scene elements into the video embeddings, enhancing them to emphasize fine-grained and salient details. For textual debiasing, we introduce a mechanism to disentangle text features into content and bias components, enabling the model to focus on meaningful content while separately handling biased information. Extensive experiments and ablation studies across five major TVR benchmarks (i.e., MSR-VTT, MSVD, LSMDC, ActivityNet, and DiDeMo) demonstrate the competitive performance of BiMa. Additionally, the model’s bias mitigation capability is consistently validated by its strong results on out-of-distribution retrieval tasks.

## 1. Introduction

The task of retrieving videos based on textual queries and vice versa, known as text-video retrieval (TVR), has rapidly evolved within multimedia information retrieval due to significant advancements in large-scale pre-trained Vision-Language Models (VLMs) such as CLIP [40] and BLIP [30]. Despite remarkable progress, existing TVR frameworks, including TeachCLIP [49], TextProxy [56], and NarVid [16], largely ignore the underlying visual-linguistic representation biases intrinsic to both the training data and pre-trained VLMs [36, 44, 45]. Representation biases are systematic deviations in datasets causing models to overemphasize specific features or patterns rather than generalizable and task-relevant aspects [36, 45]. Liu et al. [36] demonstrate that models tend to depend excessively

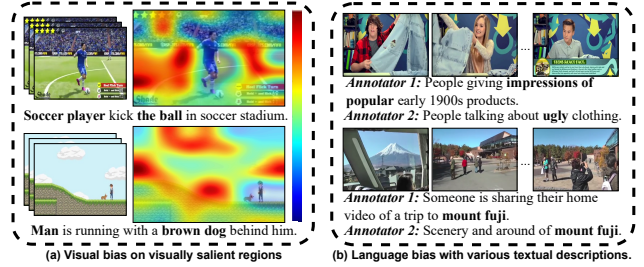


Figure 1. **Illustration of Visual-Linguistic Bias in TVR.** (a) Visual Bias: For each example, video (left of the 1<sup>st</sup> row), the associated visual feature map (right of the 1<sup>st</sup> row) extracted by pre-trained CLIP [31] and its corresponding Textual query (2<sup>nd</sup> row). This highlights a bias toward visually dominant regions while overlooking main actors/objects and activities when they occupy smaller regions in the scene. (b) Textual Bias: For each example, video (1<sup>st</sup> row) and their corresponding textual descriptions (2<sup>nd</sup> row) from various annotators, capturing emotional responses and personal perspectives.

on prominent visual concepts and dataset-specific textual patterns, resulting in representations that are tuned to the dataset rather than capturing robust, semantic-rich features. This bias limits the models’ ability to generalize to diverse, unseen scenarios. Moreover, the precise nature of the biases learned by neural networks remains largely unclear—some may even contain generalizable and transferable patterns that are not immediately apparent to human observers. Shvetsova et al. [45] also confirm that most video datasets are heavily focused on visually salient concepts, such as object bias. Thus, The absence of bias mitigation within the existing learned TVR frameworks can lead to limitations, resulting in suboptimal performance when exposed to unseen data. We proceed to further describe the bias problem in TVR.

**Visual-Linguistic Biases.** Widely-use TVR datasets such as MSR-VTT [57], MSVD [3], LSMDC [41], ActivityNet [25], and DiDeMo [13] often present practical challenges stemming from what we identify as visual-linguistic biases. These biases arise because each dataset is typically created with specific objectives that align with particular research

goals, applications, or target users. These biases are variations in visual and textual representations that can skew pre-trained models towards focusing on subjective or dataset-specific features, potentially causing them to overlook essential factual information. The visual-linguistic bias problem can be partitioned into two sub-problems: visual bias and textual bias, as follows.

Visual bias primarily arises due to coarse-grained annotations that often omit critical details such as key actors, objects, or their interactions. Consequently, visual embeddings produced by pre-trained encoders frequently emphasize visually dominant areas, neglecting smaller but semantically crucial components. Figure 1(a) illustrates this issue, showing how pre-trained CLIP disproportionately focuses on the larger environmental context, marginalizing important yet smaller elements such as the “man” and “brown dog,” crucial to understanding the scene.

Textual bias occurs when annotators’ subjective interpretations, cultural perspectives, emotional states, or language usage differences produce varying textual descriptions for identical video scenes. This variability causes models to capture subjective rather than objective semantic content. As depicted in Figure 1(b), distinct annotators produce emotionally and culturally varied descriptions, demonstrating the need for effective textual bias neutralization.

To address the aforementioned visual-linguistic bias problem, we propose *Bias Mitigation Text-Video Retrieval (BiMa)*. The BiMa’s objectives are twofold: (i) neutralize visual-linguistic biases and (ii) enhance the model’s focus on relevant features. To obtain these goals, BiMa is equipped with three key modules—(i) *Scene Element Construction*, (ii) *Visual Scene Debias*, and (iii) *Textual Content Debias*. The *Scene Element Construction* module aggregates fine-grained entities and actions, providing structured semantic guidance. Subsequently, the *Visual Scene Debias* module leverages these elements to reorient visual attention toward essential components, thus reducing visual bias. The *Textual Content Debias* module employs a novel disentanglement mechanism to separate textual content from bias-induced variations, ensuring semantic consistency across diverse annotations. Critically, this mechanism is self-supervised, obviating the need for expensive additional annotations. Finally, to further evaluate our proposed bias mitigation framework, out-of-domain retrieval experiments are leveraged to validate the efficacy and assess the generalization of models beyond training-specific biases by evaluating performance across distinctly different datasets or scenarios, such as training on MSR-VTT and testing on ActivityNet Captions. In summary, our contributions are:

- Explicitly identifying and defining visual-linguistic biases in TVR task, drawing upon recent bias representation findings [36, 45].
- Proposing BiMa, a systematic framework for bias mitiga-

tion with three integrated modules: *Scene Element Construction*, *Visual Scene Debias*, and *Textual Content Debias*.

- Achieving state-of-the-art performance and robust generalization across multiple TVR benchmarks (MSR-VTT, MSVD, LSMDC, ActivityNet Captions, DiDeMo), supported by comprehensive ablation studies and significant bias reduction in out-of-domain retrieval settings.

## 2. Problem Definition

**Text-Video Retrieval.** Given a text query  $\mathbf{T}^{(i)} = \langle \mathbf{T}_1^{(i)}, \mathbf{T}_2^{(i)}, \dots, \mathbf{T}_{N_t}^{(i)} \rangle$  with  $N_t$  word tokens and a video  $\mathbf{V}^{(i)} = \langle \mathbf{V}_1^{(i)}, \mathbf{V}_2^{(i)}, \dots, \mathbf{V}_{N_f}^{(i)} \rangle$  with  $N_f$  frames. A Text Encoder encodes  $\mathbf{T}^{(i)}$  into a sequence of  $N_t + 1$  word embeddings  $\mathbf{t}^{(i)} = \langle \mathbf{t}_1^{(i)}, \mathbf{t}_2^{(i)}, \dots, \mathbf{t}_{N_t}^{(i)}, \mathbf{t}_{[\text{CLS}]}^{(i)} \rangle$ , where  $\mathbf{t}_{[\text{CLS}]}$  is the global textual embedding. A Video Encoder encodes  $\mathbf{V}^{(i)}$  into a sequence of  $N_f$  frame embedding  $\mathbf{v}^{(i)} = \langle \mathbf{v}_1^{(i)}, \mathbf{v}_2^{(i)}, \dots, \mathbf{v}_{N_f}^{(i)} \rangle$ . We aim to learn a cross-modality similarity measure that assigns a high similarity score to  $\mathbf{V}^{(i)}$  and  $\mathbf{T}^{(i)}$  and a low similarity score to  $\mathbf{V}^{(j)}$  (with  $j \neq i$ ) and  $\mathbf{T}^{(i)}$ . Equation 1 formally defines the TVR problem. For brevity, we only focus on the Text-to-Video (T2V). The Video-to-Text (V2T) can be similarly defined.

$$\max s(\mathbf{V}^{(i)}, \mathbf{T}^{(i)}) = \max \mathbb{P}(\mathbf{V}^{(i)} | \mathbf{T}^{(i)}) = \max \mathbb{P}(\mathbf{v}^{(i)} | \mathbf{t}^{(i)}) \quad (1)$$

Here,  $s(\cdot, \cdot)$  is a *cosine* similarity and  $\mathbb{P}(\cdot | \cdot)$  indicates the conditional probability.

**Visual-Linguistic Biases.** When *visual bias* occurs, the visual embedding features of a video  $\mathbf{V}^{(i)}$  differ from the matching visual embedding features generated for a corresponding query  $\mathbf{T}^{(i)}$ . We define the visual bias as follows.

$$\mathbb{P}(\mathbf{v}^{(i)} | \mathbf{V}^{(i)}) \neq \mathbb{P}(\mathbf{v}^{(i)} | \mathbf{T}^{(i)}) \Rightarrow \mathbb{P}(\mathbf{v}^{(i)} | \mathbf{V}^{(i)}) \neq \mathbb{P}(\mathbf{v}^{(i)} | \mathbf{t}^{(i)}) \quad (2)$$

Equation 2 indicates that the Video Encoder does not provide the matching visual embedding features. When a pre-trained model is used as the Video Encoder, the bias can lean towards the pre-trained features.

When *textual bias* occurs, the probability of the visual embedding features given the textual biases ( $\tilde{\mathbf{t}}^{(i)}$ ) is higher than the visual embedding given the true semantic textual features ( $\hat{\mathbf{t}}^{(i)}$ ). We define the textual bias as follows.

$$\mathbb{P}(\mathbf{v}^{(i)} | \tilde{\mathbf{t}}^{(i)} + \hat{\mathbf{t}}^{(i)}) > \mathbb{P}(\mathbf{v}^{(i)} | \hat{\mathbf{t}}^{(i)}) \Rightarrow \mathbb{P}(\mathbf{v}^{(i)} | \mathbf{t}^{(i)}) \neq \mathbb{P}(\mathbf{v}^{(i)} | \tilde{\mathbf{t}}^{(i)}) \quad (3)$$

Equation 3 indicates that the similarity between the visual embedding features and the textual biases is higher than the similarity between the visual embedding features and the true semantic textual features.

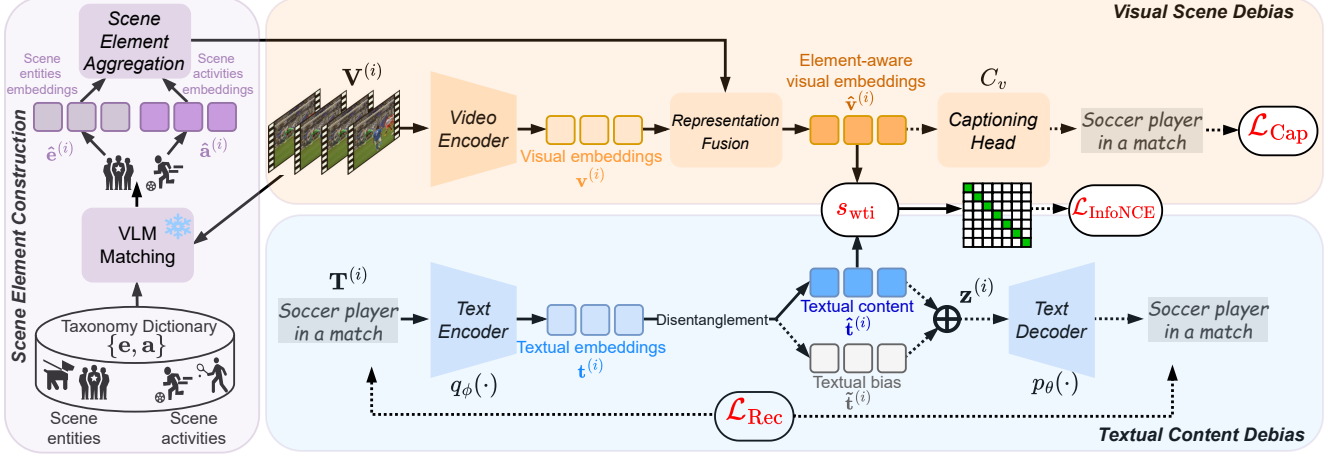


Figure 2. **Overview of BiMa.** The dashed line represents the model flow used exclusively during training, while the solid line indicates usage in both training and inference.

### 3. Methodology

Figure 2 shows the the framework overview, comprising of three main modules: (i) *Scene Element Construction*, (ii) *Visual Scene Debias*, and (iii) *Textual Content Debias*. We proceed to introduce these modules in the following sections.

#### 3.1. Scene Element Construction

*Scene Element Construction* aims to generate scene elements for each video and the corresponding embeddings. In our proposed framework, scene elements play a central role in debiasing across different modalities. Scene elements consist of scene entities (noun phrases representing actors or objects) and scene activities (verb phrases representing behaviors or actions), which are drawn from a comprehensive scene taxonomy dictionary (detailed implementation is presented in the **Supplementary Material**). Formally, scene elements are represented as a set of nouns and verb phrases  $\{e, a\}$  that is extracted from large-scale text-video descriptions.

**Scene Elements Generation.** Given a video  $V^{(i)}$ , we leverage the zero-shot capability of a pre-trained CLIP model with frozen weights to perform text-video matching to identify the most relevant scene elements. In particular, we use CLIP’s textual encoder to obtain global textual tokens including a set of  $N_e$  scene entities  $e = \{e^{(i)}\}_{i=1}^{N_e}$ , and a set of  $N_a$  scene activities  $a = \{a^{(i)}\}_{i=1}^{N_a}$ . Simultaneously, we feed  $V^{(i)}$  into CLIP’s visual encoder to obtain frame-level visual feature embeddings  $v^{(i)}$ . The embeddings  $v^{(i)}$  are then temporally aggregated through mean pooling to yield a video-level representation  $\bar{v}^{(i)}$ . Then, we calculate the similarity between  $\bar{v}^{(i)}$  with scene entities dictionary  $e$  and scene activities dictionary  $a$ . After that, we select the top- $\kappa$  relevant scene entities  $\hat{e}^{(i)} = \langle \hat{e}_1^{(i)}, \hat{e}_2^{(i)}, \dots, \hat{e}_\kappa^{(i)} \rangle$  and top- $\kappa$  scene activities  $\hat{a}^{(i)} = \langle \hat{a}_1^{(i)}, \hat{a}_2^{(i)}, \dots, \hat{a}_\kappa^{(i)} \rangle$  with the highest

similarity scores as “scene elements” of  $V^{(i)}$ .

**Scene Elements Aggregation.** To enhance the discriminative features corresponding to  $V^{(i)}$ , we combine scene entities and scene activities into a unified scene element embedding  $c^{(i)}$ . Specifically, we introduce a balancing coefficient  $g$  that adjusts the relative importance of scene entities  $\hat{e}^{(i)}$  and scene activities  $\hat{a}^{(i)}$  for each video  $V^{(i)}$ . This coefficient  $g$  supports a smooth aggregation of embeddings by establishing an association between each feature token and its most relevant counterpart among the other feature tokens. The formulation of  $g$  is provided in Equation 4.

$$g_{(\hat{a}^{(i)}, \hat{e}^{(i)})} = 1 - \frac{1}{\kappa} \sum_l \max_j [s(\hat{a}_l^{(i)}, \hat{e}_j^{(i)})_{j=1}^\kappa] \quad (4)$$

Here,  $s(\cdot)$  indicates the *cosine* similarity. The coefficient  $g$  is then used to aggregate  $\hat{e}^{(i)}$  and  $\hat{a}^{(i)}$  to obtain scene element embeddings  $c^{(i)}$  as follows.

$$c^{(i)} = \hat{a}^{(i)} \oplus g_{(\hat{a}^{(i)}, \hat{e}^{(i)})} \cdot \hat{e}^{(i)} \quad (5)$$

Here,  $\oplus$  indicates the element-wise summation operation.

#### 3.2. Visual Scene Debias

*Visual Scene Debias* module aims to mitigate visual biases by explicitly emphasizing fine-grained semantic contents in the visual representation. Particularly, it leverages scene elements to produce element-aware visual scene embeddings. Formally, we aim to mitigate the problem  $\mathbb{P}(v^{(i)}|V^{(i)}) \neq \mathbb{P}(v^{(i)}|t^{(i)})$  (see Equation 2) by augmenting the visual embedding  $v^{(i)}$  with the scene element  $c^{(i)}$  to obtain the augmented visual feature  $\hat{v}^{(i)}$ . Then,  $\hat{v}^{(i)}$  is employed as the feature for matching such that  $\mathbb{P}(\hat{v}^{(i)}|V^{(i)}) \approx \mathbb{P}(\hat{v}^{(i)}|t^{(i)})$ . We elaborate on this in the following sections.

**Cross-modality Debias via Representation Fusion.** Debiasing visual representations involves generating element-aware visual scene embeddings that emphasize relevant information at a lower-dimensional latent space, while capturing interactions between cross-modal features. More specifically, we aim to align the video embeddings  $\mathbf{v}^{(i)}$  and scene element embeddings  $\mathbf{c}^{(i)}$  to highlight the relevant information  $\hat{\mathbf{v}}^{(i)}$  of the video  $\mathbf{V}^{(i)}$ . First, we compute an attention map between a query  $\mathbf{q}_v$ , a key  $\mathbf{k}_c$ , and a value  $\mathbf{v}_c$ . Here,  $\mathbf{q}_v$  represents video embeddings  $\mathbf{v}^{(i)}$ , and both  $\mathbf{k}_c$  and  $\mathbf{v}_c$  represent scene element embeddings  $\mathbf{c}^{(i)}$ . Then, element-aware visual scene features  $\hat{\mathbf{v}}^{(i)}$  are computed through a cross-attention layer [52] as shown in Equation 6.

$$\mathbf{q}_v = \text{Linear}(\mathbf{v}^{(i)}), \mathbf{k}_c = \text{Linear}(\mathbf{c}^{(i)}), \mathbf{v}_c = \text{Linear}(\mathbf{c}^{(i)}),$$

$$\hat{\mathbf{v}}^{(i)} = \text{softmax} \left( \frac{\mathbf{q}_v \mathbf{k}_c^\top}{\sqrt{d}} \right) \mathbf{v}_c.$$

### Fine-grained Semantic Learning with Captioning Head.

Inspired by CoCa [62] that leverages captioning for salient semantic pretraining, we propose to additionally adopt a *Captioning Head*  $C_v(\cdot)$  parameterized by a stack of  $M$  transformer decoders to further learn cross-modal details within element-aware visual scene embeddings  $\hat{\mathbf{v}}^{(i)}$ . In other words, on top of contrastive matching with textual embeddings, the element-aware visual scene embeddings are learned via a text-generative decoding process. At each decoding step,  $C_v(\cdot)$  is trained to predict the subsequent text token  $\mathbf{T}_l^{(i)}$  with the highest log-likelihood. Thus, it learns to auto-regressively maximize the log-likelihood of predicting the input’s textual token  $\mathbf{T}_l^{(i)}$  based on previous tokens  $\mathbf{T}_{0:l-1}^{(i)}$ . As  $C_v(\cdot)$  relies on  $\hat{\mathbf{v}}^{(i)}$ , the embeddings  $\hat{\mathbf{v}}^{(i)}$  can be established at a deeper alignment of cross-modal representation via Equation 6.

$$\mathcal{L}_{\text{Cap}} = \sum_{l=1}^{N_t} -\log C_v(\mathbf{T}_l^{(i)} | \mathbf{T}_{0:l-1}^{(i)}, \hat{\mathbf{v}}^{(i)}). \quad (6)$$

### 3.3. Textual Content Debias

*Textual Content Debias* aims to detach the textual bias from the description and encourage the model to capture the true semantic features via a disentanglement process. Formally, we aim to solve the problem  $\mathbb{P}(\mathbf{v}^{(i)} | \mathbf{t}^{(i)}) \neq \mathbb{P}(\mathbf{v}^{(i)} | \hat{\mathbf{t}}^{(i)})$  (Equation 3) by repurposing the *Text Encoder* to decompose every textual description  $\mathbf{T}^{(i)}$  into a true semantic component  $\hat{\mathbf{t}}^{(i)}$  and a textual bias component  $\tilde{\mathbf{t}}^{(i)}$ . Then,  $\hat{\mathbf{t}}^{(i)}$  is employed as the textual feature for matching with the augmented element-aware visual scene features  $\hat{\mathbf{v}}^{(i)}$  which is obtained from the *Visual Scene Debias*, such that  $\mathbb{P}(\mathbf{v}^{(i)} | \mathbf{t}^{(i)}) \approx \mathbb{P}(\hat{\mathbf{v}}^{(i)} | \hat{\mathbf{t}}^{(i)})$ . We elaborate on this in the below sections.

**Content-Bias Representation Disentanglement.** Motivated by the disentanglement ability of  $\beta$ -VAE frame-

work [14], we propose to use *Text Encoder* to decompose the original textual content  $\mathbf{T}^{(i)}$  into two parts in the latent space: a textual content component  $\hat{\mathbf{t}}^{(i)}$  and the textual bias component  $\tilde{\mathbf{t}}^{(i)}$ . These two parts are learned under completely different constraints, thereby separating their representations. The former is aligned with the element-aware visual scene features  $\hat{\mathbf{v}}^{(i)}$  to enable content matching. The latter is modeled as a stochastic representation following a Gaussian distribution with the mean ( $\mu$ ) and variance ( $\sigma^2$ ). By doing this, we aim to handle biases as Gaussian noise. Combining both components will result in the latent representation  $\mathbf{z}^{(i)} = \hat{\mathbf{t}}^{(i)} + \tilde{\mathbf{t}}^{(i)}$ . Then, the obtained latent representation  $\mathbf{z}^{(i)}$  is employed to reconstruct the original textual description  $\mathbf{T}^{(i)}$ . By reconstructing the two separate components, we ensure the complementary property of each component. In other words, we ensure the combination resulting in  $\mathbf{z}^{(i)}$  is meaningful. The reconstruction closely follows the ELBO formulation from conventional VAE framework [24], which optimizes the variational lower bound on data log-likelihood as shown in Equation 7.

$$\mathcal{L}_{\text{VAE}} = \underbrace{-\mathbb{E}_{\mathbf{z}^{(i)} \sim q_\phi(\mathbf{z}^{(i)} | \mathbf{T}^{(i)})} [\log p_\theta(\mathbf{T}^{(i)} | \mathbf{z}^{(i)})]}_{\mathcal{L}_{\text{Rec}}} + \underbrace{D_{\text{KL}}(q_\phi(\mathbf{z}^{(i)} | \mathbf{T}^{(i)}) || p_\theta(\mathbf{z}^{(i)}))}_{\mathcal{L}_{\text{KL}}} \quad (7)$$

Here,  $p_\theta(\mathbf{z}^{(i)})$  is a prior modeled as  $\mathcal{N}(\mathbf{0}, \mathbf{I})$ . The conditional probability distributions  $q_\phi(\mathbf{z}^{(i)} | \mathbf{T}^{(i)})$ ,  $p_\theta(\mathbf{T}^{(i)} | \mathbf{z}^{(i)})$  are estimated by the *Text Encoder* and *Text Decoder* networks, respectively. Here,  $\mathbf{z}^{(i)}$  plays the role of textual embedding, i.e.,  $\mathbf{z}^{(i)} = \mathbf{t}^{(i)}$ . Next,  $D_{\text{KL}}(\cdot, \cdot)$  is the Kullback-Leibler (KL) divergence aiming to enforce the posterior and the prior distribution to be close to each other. The KL divergence plays as a disentanglement factor to enforce the disentanglement process of the bias from the original textual features. Also, it serves as a regularizer that prevents the latent representation from collapsing to zero. The reconstruction term  $\mathcal{L}_{\text{Rec}}$  in the VAE loss measures the log-likelihood of *Text Decoder*  $p_\theta$  to auto-regressively reconstruct the ground-truth input’s textual description  $\mathbf{T}^{(i)}$  as defined in Equation 8.

$$\mathcal{L}_{\text{Rec}} = \sum_{l=1}^{N_t} -\log p_\theta(\mathbf{T}_l^{(i)} | \mathbf{T}_{0:l-1}^{(i)}, \mathbf{z}^{(i)}). \quad (8)$$

To capture the unpredictable variations of the textual biases, we model  $\tilde{\mathbf{t}}^{(i)}$  as a probabilistic representation. While these features are not explicitly matched to visual representations, they act as distractors for TVR and thus must be modeled to facilitate effective disentanglement. Following this insight, we model the latent representation  $\tilde{\mathbf{t}}^{(i)}$  as a multivariate Gaussian distribution.

$$q_\phi(\tilde{\mathbf{t}}^{(i)} | \mathbf{T}^{(i)}) \sim \mathcal{N}(\mu, \text{diag}(\sigma^2)) \quad (9)$$



To ensure stable training, we apply the reparameterization trick as formulated in Equation 10.

$$q_\phi(\tilde{\mathbf{t}}^{(i)}|\mathbf{T}^{(i)}) = \mu + \sigma \cdot \epsilon, \quad (10)$$

where  $\epsilon$  is an auxiliary noise variables and  $\epsilon \sim \mathcal{N}(\mathbf{0}, \mathbf{I})$ .

After modeling the latent representation of textual biases as a distribution  $q_\phi(\tilde{\mathbf{t}}^{(i)}|\mathbf{T}^{(i)})$ , we generate textual bias embedding  $\tilde{\mathbf{t}}^{(i)}$  by sampling  $K$  instances from this distribution during the training process as shown in Equation 11. This process allows for gradient propagation through the sampled embeddings of bias modeling.

$$\tilde{\mathbf{t}}^{(i)} = \langle \tilde{\mathbf{t}}_1^{(i)}, \dots, \tilde{\mathbf{t}}_2^{(i)}, \tilde{\mathbf{t}}_K^{(i)} \rangle \sim q_\phi(\tilde{\mathbf{t}}^{(i)}|\mathbf{T}^{(i)}) \quad (11)$$

**Element-Aware Content Learning by Alignment.** Our framework performs disentanglement between content and bias representations by explicitly matching the content embeddings with element-aware visual embeddings, and performing reconstruction of textual disentanglement. In particular, our model is trained via contrastive alignment between element-aware visual embeddings  $\hat{\mathbf{v}}^{(i)}$  and textual content embeddings  $\tilde{\mathbf{t}}^{(i)}$  to optimize their cross-modal similarity (see Equation 12). Meanwhile, the original texts  $\mathbf{t}^{(i)}$  are disentangled as content  $\hat{\mathbf{t}}^{(i)}$  and bias  $\tilde{\mathbf{t}}^{(i)}$ , and reconstructed via  $\mathbf{z}^{(i)}$  and  $\mathcal{L}_{\text{VAE}}$ . Thus, by the process of elimination, we capture bias representations  $\tilde{\mathbf{t}}^{(i)}$  as residual information that is less relevant to element-aware visual embeddings  $\hat{\mathbf{v}}^{(i)}$ , yet are part of the original information  $\mathbf{t}^{(i)}$ .

### 3.4. Objective Function

To enhance the model’s ability to discern relevant features within the data, we replace mean pooling with an advanced weighted pooling mechanism termed Weighted Token Interaction (WTI) [34] in order to learn the token-level interaction between cross-modal embeddings. The token-level matching function is denoted as  $s_{\text{wti}}(\cdot)$ .

For contrastive learning, we adopt the InfoNCE loss function [50] to optimize cross-modal similarity between  $\hat{\mathbf{v}}^{(i)}$  and  $\hat{\mathbf{t}}^{(j)}$  of two sample  $i$  and  $j$  as shown in Equation 12.

$$\begin{aligned} \mathcal{L}_{\text{InfoNCE}} = & -\frac{1}{2B} \sum_{i=1}^B \log \frac{\exp(s_{\text{wti}}(\hat{\mathbf{v}}^{(i)}, \hat{\mathbf{t}}^{(i)}) \cdot \tau)}{\sum_{j=1}^B \exp(s_{\text{wti}}(\hat{\mathbf{v}}^{(j)}, \hat{\mathbf{t}}^{(i)}) \cdot \tau)} \\ & -\frac{1}{2B} \sum_{i=1}^B \log \frac{\exp(s_{\text{wti}}(\hat{\mathbf{v}}^{(i)}, \hat{\mathbf{t}}^{(i)}) \cdot \tau)}{\sum_{j=1}^B \exp(s_{\text{wti}}(\hat{\mathbf{v}}^{(i)}, \hat{\mathbf{t}}^{(j)}) \cdot \tau)}, \end{aligned} \quad (12)$$

where  $\tau$  is a learnable scaling factor and  $B$  is the batch size.

Our process to mitigate visual-linguistic biases exhibits during both training and inference by our end-to-end architecture. However, bias modeling is not required during the inference. The overall objective is defined in Equation 13.

$$\mathcal{L} = \mathcal{L}_{\text{InfoNCE}} + \lambda_{\text{Cap}} \cdot \mathcal{L}_{\text{Cap}} + \lambda_{\text{Rec}} \cdot \mathcal{L}_{\text{Rec}} + \lambda_{\text{KL}} \cdot \mathcal{L}_{\text{KL}} \quad (13)$$

Here,  $\lambda_{\text{cap}}$ ,  $\lambda_{\text{rec}}$ , and  $\lambda_{\text{KL}}$  are the hyperparameters that control the trade-off among three loss terms.

## 4. Experiments

### 4.1. Experimental Setups.

**Datasets.** We conducted experiments on five major TVR benchmarking datasets:

- (1) MSR-VTT [57] dataset contains 10,000 YouTube videos, with 20 descriptions per video. We follow the 1k-A split [37] to conduct training on 9,000 videos and report testing results on the other 1,000 videos.
- (2) MSVD [3] contains 1,970 videos with over 80,000 descriptions, with 40 descriptions on average per video. We follow the official split with 1,200 videos for training and 670 videos for testing.
- (3) LSMDC [41] contains 118,081 video clips, which are extracted from 202 movies. We follow the split of [8] with 100,000 videos for training and 1,000 videos for testing.
- (4) ActivityNet Captions [25] contains 20,000 YouTube videos, following the training and evaluation protocol in [37], we report results on the “val1” split of 10,009 and 4,917 as the train and test set, respectively.
- (5) DiDeMo [13] contains 10,464 videos with over 40,543 text descriptions. We follow the training and evaluation protocol in [37].

These datasets vary in video duration, research goals, target users, and text annotations, providing a comprehensive evaluation of different methods. We evaluate the Text→Video (T2V) performance and provide additional results of Video→Text (V2T) performance on standard rank-based metrics *i.e.* Recall at top {1, 5, 10} (recall at rank 1, 5, 10), Rsum (R@1 + R@5 + R@10).

**Implementation Details.** We use CLIP ViT/B-32 as the backbone for both *Video Encoder* and *Text Encoder*. We set  $N_t = 32$  and  $N_f = 32$  as the number of word tokens and video frames for all datasets except DiDeMo and ActivityNet, where  $N_t$  and  $N_f$  are set to 64. We train with batch size of 128 for 5 epochs, except for DiDeMo with 10 epochs and ActivityNet with 20 epochs. We use the Adam [23] as the optimizer. The learning rate follows the cosine schedule with a linear warmup strategy [11]. For Equation 4, we set  $\kappa = 20$ . For Equation 13, We set  $\lambda_{\text{cap}} = 0.3$ ,  $\lambda_{\text{rec}} = 0.5$ , and  $\lambda_{\text{KL}} = 1e^{-4}$ .

### 4.2. Quantitative Results

**Comparison with SOTA.** We compare the proposed BiMa with SOTA methods. Table 1 shows the retrieval results on the MSR-VTT dataset, where our proposed method attains SOTA on both T2V and V2T tasks. We achieve 53.5 in the T2V task, outperforming the runner-up TextProxy [56] by 1.2 and the third best DITS [54] by 1.6 w.r.t. R@1. On other metrics, BiMa also significantly outperforms the runner-up

Table 1. **T2V** and **V2T** performance comparisons on MSR-VTT dataset. The best and second best are **bold** and underlined. Two-stage methods are marked with †.

PT	Methods	T2V				V2T			
		R@1↑	R@5↑	R@10↑	Rsum↑	R@1↑	R@5↑	R@10↑	Rsum↑
✓	ClipBERT [27] CVPR'20	22.0	46.8	59.9	128.7	-	-	-	-
	SupportSet [38] ICLR'21	30.1	58.5	69.3	157.9	28.5	58.6	71.6	158.7
	Frozen [1] ICCV'21	32.5	61.5	71.2	165.2	-	-	-	-
	TMVM [33] NeurIPS'22	36.2	64.2	75.7	176.1	34.8	63.8	73.7	172.3
	RegionLearner [59] AAAI'23	36.3	63.9	72.5	172.7	34.3	63.5	73.2	171.0
	In-Style [44] ICCV'23	36.2	61.8	71.9	169.9	-	-	-	-
✗	CenterCLIP [64] SIGIR'22	44.2	71.6	82.1	197.9	42.8	71.7	82.2	196.7
	CLIP4Clip [37] Neurocomputing'22	44.5	71.4	81.6	197.5	42.7	70.9	80.6	194.2
	EMCL-Net [18] NeurIPS'22	46.8	73.1	83.1	203.0	46.5	73.5	83.5	203.5
	X-Pool [10] CVPR'22	46.9	72.8	82.2	201.9	-	-	-	-
	TS2-Net [35] ECCV'22	47.0	74.5	83.8	205.3	45.3	74.1	83.7	203.1
	HBI [19] CVPR'23 †	48.6	74.6	83.4	206.6	46.8	74.3	84.3	205.4
	DiCoSa [20] IJCAI'23	47.5	74.7	83.8	206.0	46.7	75.2	84.3	206.2
	UATVR [7] ICCV'23	47.5	73.9	83.5	204.9	46.9	73.8	83.8	204.5
	DiffusionRet [21] ICCV'23 †	49.0	75.2	82.7	206.9	47.7	73.8	84.5	206.0
	PAU [21] NeurIPS'23	48.5	72.7	82.5	203.7	48.3	73.0	83.2	204.5
	DGL [61] AAAI'24	45.8	69.3	79.4	194.5	-	-	-	-
	EERCF [6] AAAI'24	47.8	74.1	84.1	206.0	44.7	74.2	83.9	202.8
	TeachCLIP [49] CVPR'24	46.8	74.3	82.6	203.7	-	-	-	-
	DITS [54] NeurIPS'24	51.9	75.7	84.6	212.2	-	-	-	-
	TextProxy [56] AAAI'25	<u>52.3</u>	<u>77.8</u>	<u>85.8</u>	<u>215.9</u>	-	-	-	-
	TempMe [43] ICLR'25	46.1	71.8	80.7	198.6	45.6	72.4	81.2	199.2
	NarVid [16] CVPR'25	51.0	76.4	85.2	212.6	<u>50.0</u>	<u>75.4</u>	<u>83.8</u>	<u>209.2</u>
	<b>BiMa (ours)</b>	<b>53.5</b>	<b>78.6</b>	<b>86.5</b>	<b>218.6</b>	<b>52.2</b>	<b>77.1</b>	<b>85.3</b>	<b>214.6</b>

Table 2. **T2V** comparisons on MSVD, LSMDC, ActivityNet, and DiDeMo datasets. The best and second best are **bold** and underlined.

Methods	MSVD				LSMDC				ActivityNet				DiDeMo			
	R@1↑	R@5↑	R@10↑	Rsum↑	R@1↑	R@5↑	R@10↑	Rsum↑	R@1↑	R@5↑	R@10↑	Rsum↑	R@1↑	R@5↑	R@10↑	Rsum↑
ClipBERT	-	-	-	-	-	-	-	-	21.3	49.0	63.5	133.8	20.4	48.0	60.8	129.2
SupportSet	28.4	60.0	72.9	161.3	-	-	-	-	29.2	61.6	94.7	185.5	-	-	-	-
Frozen	33.7	64.7	76.3	174.7	15.0	30.8	40.3	86.1	-	-	-	-	34.6	65.0	74.7	174.3
TMVM	36.7	67.4	81.3	185.4	17.8	37.1	45.9	100.8	-	-	-	-	36.5	64.9	75.4	176.8
RegionLearner	44.0	74.9	84.3	203.2	17.1	32.5	41.5	91.1	-	-	-	-	32.5	60.8	72.3	165.6
In-Style	44.8	72.5	81.2	198.5	16.1	33.6	39.7	89.4	-	-	-	-	32.1	61.9	71.2	165.2
CenterCLIP	45.2	75.5	84.3	205.0	22.6	41.0	49.1	112.7	40.5	72.4	83.6	196.5	42.8	68.5	79.2	190.5
CLIP4Clip	45.2	75.5	84.3	205.0	22.6	41.0	49.1	112.7	40.5	72.4	83.6	196.5	42.8	68.5	79.2	190.5
EMCL-Net	42.1	71.3	81.1	194.5	23.9	42.4	50.9	117.2	41.2	72.7	83.6	197.5	45.3	74.2	82.3	201.8
X-Pool	47.2	77.4	86.0	210.6	25.2	43.7	53.5	122.4	-	-	-	-	-	-	-	-
TS2-Net	-	-	-	-	23.4	42.3	50.9	116.6	41.0	73.6	84.5	199.1	41.8	71.6	82.0	195.4
HBI	-	-	-	-	-	-	-	-	42.2	73.0	84.6	199.8	46.9	74.9	82.7	204.5
DiCoSa	47.4	76.8	86.0	210.2	25.4	43.6	54.0	123.0	42.1	73.6	84.6	200.3	45.7	74.6	83.5	203.8
UATVR	46.0	76.3	85.1	207.4	-	-	-	-	-	-	-	-	43.1	71.8	82.3	197.2
DiffusionRet	46.6	75.9	84.1	206.6	24.4	43.1	54.3	121.8	45.8	75.6	86.3	207.7	46.7	74.7	82.7	204.1
PAU	47.3	77.4	85.5	210.2	-	-	-	-	-	-	-	-	48.6	76.0	84.5	209.1
EERCF	47.0	77.5	85.4	209.9	-	-	-	-	43.1	74.5	86.0	203.6	-	-	-	-
DGL	-	-	-	-	21.4	39.4	48.4	109.2	38.6	69.2	81.6	189.4	-	-	-	-
TeachCLIP	47.4	77.3	85.5	210.2	-	-	-	-	42.2	72.7	85.2	200.1	43.7	71.2	81.1	196.0
DITS	-	-	-	-	<u>28.2</u>	<u>47.3</u>	<u>56.6</u>	<u>132.1</u>	-	-	-	-	51.1	77.9	85.8	214.8
TextProxy	-	-	-	-	-	-	-	-	<u>53.0</u>	<u>80.9</u>	<u>89.6</u>	<u>223.5</u>	50.6	76.9	86.0	213.5
TempMe	-	-	-	-	23.5	41.7	51.8	117.0	44.9	75.2	85.5	205.6	48.0	72.4	81.8	202.2
NarVid	53.1	81.4	88.8	223.3	-	-	-	-	-	-	-	-	<u>53.4</u>	<u>79.1</u>	<u>86.3</u>	<u>218.8</u>
<b>BiMa (ours)</b>	<b>55.7</b>	<b>83.2</b>	<b>91.2</b>	<b>230.1</b>	<b>35.6</b>	<b>56.5</b>	<b>68.1</b>	<b>160.2</b>	<b>55.4</b>	<b>83.4</b>	<b>92.4</b>	<b>231.2</b>	<b>56.0</b>	<b>81.9</b>	<b>87.8</b>	<b>225.7</b>

Table 3. **Out-of-distribution** performance of **T2V** models on LSMDC, ActivityNet, and DiDeMo. The best and second-best results are highlighted in **bold** and underlined, respectively.

Methods	MSR-VTT → LSMDC				MSR-VTT → ActivityNet				MSR-VTT → DiDeMo			
	R@1↑	R@5↑	R@10↑	Rsum↑	R@1↑	R@5↑	R@10↑	Rsum↑	R@1↑	R@5↑	R@10↑	Rsum↑
CLIP4Clip	15.3	31.3	40.5	87.1	29.1	58.3	72.1	159.5	31.8	57.0	66.1	154.9
EMCL-Net	16.6	29.3	36.5	82.4	28.7	56.8	70.6	156.1	30.0	56.1	65.8	151.9
DiffusionRet	17.1	32.4	41.0	90.5	31.5	60.0	73.8	165.3	33.2	59.3	68.4	160.9
<b>BiMa (ours)</b>	<b>24.0</b>	<b>45.0</b>	<b>56.8</b>	<b>125.8</b>	<b>35.2</b>	<b>64.8</b>	<b>89.0</b>	<b>189.0</b>	<b>36.7</b>	<b>62.6</b>	<b>71.2</b>	<b>170.5</b>

results. In **V2T** task, we achieve 52.2, outperforming the runner-up NarVid [16] by 2.2 w.r.t. R@1. Table 2 shows the

retrieval results on **T2V**, where BiMa consistently achieves the best results on all the metrics on all four datasets MSVD,

Table 4. T2V ablation studies for network designs on MSR-VTT. Exp #1 is our baseline which is CLIP4Clip with WTI matching.

Exp	Visual Scene Debias			Textual Content Debias	Performance		
	Scene Element Entities	Scene Activities	Captioning Head		R@1↑	R@5↑	R@10↑
#1	✗	✗	✗	✗	45.7	73.0	82.6
#2	✓	✗	✗	✗	49.2	75.3	83.0
#3	✗	✓	✗	✗	49.4	75.7	83.4
#4	✓	✓	✗	✗	51.5	76.6	84.8
#5	✓	✓	✓	✗	52.1	77.2	86.0
#6	✗	✗	✗	✓	47.0	75.8	84.0
#7	✓	✓	✓	✓	53.5	78.6	86.5

LSMDC, ActivityNet, and DiDeMo. It demonstrates that our strategy can work well across different domains and different text-video data variations, thus underscoring the efficacy of BiMa through the “Visual-Linguistic Bias Mitigation” technique. For example, on MSVD, our approach at 55.7 has outperformed the recent SOTA method NarVid [16] by 2.6 w.r.t R@1. Similarly on ActivityNet, BiMa significantly outperforms the runner-up TextProxy by 2.4 and w.r.t R@1, achieving SOTA performance of 55.4.

**Generalization to Unseen Domains.** Our mitigation of visual-linguistic biases is geared towards maximizing the quality of cross-modal semantic representations during training, thereby capturing better underlying patterns that can generalize to unseen data. Hence, to evaluate BiMa’s debias capability, we evaluate BiMa on out-of-distribution retrieval settings [4] (denoted as  $A \rightarrow B$ ) where the model is trained on dataset A and benchmarked on dataset B, which is unseen during training. In Table 3, we compare our BiMa with recent SOTAs and the baseline CLIP4Clip in three OOD retrieval benchmarks (MSR-VTT  $\rightarrow$  LSMDC, MSR-VTT  $\rightarrow$  ActivityNet, and MSR-VTT  $\rightarrow$  DiDeMo) where BiMa significantly outperforms others on the three benchmarks. These results suggest that our bias mitigation capability supports model generalization and transfer to unseen data.

**Hyperparameter Sensitivity.** In Figure 3, we evaluate hyperparameters  $\lambda_{Cap} \in [0.1, 0.5]$ ,  $\lambda_{Rec} \in [0.3, 0.7]$  and  $\lambda_{KL} \in [0.0001, 0.0005]$ . In Figure 3(left), BiMa achieves highest R@1 score when  $\lambda_{Cap} = 0.3$  for T2V. As a result, we select  $\lambda_{Cap} = 0.3$ . In Figure 3(middle), the best is achieved with  $\lambda_{Rec} = 0.5$ , so we set  $\lambda_{Rec} = 0.5$  as the default. In Figure 3(right), we show that  $\lambda_{KL}$  is highly sensitive and leads to a trade-off between T2V and V2T performance when  $\lambda_{KL}$  change from 0.0001 to 0.0003. Thus, we set  $\lambda_{KL} = 0.0001$  to balance between T2V and V2T.

**Effect of the Visual Scene Debias.** Table 4 shows that scene element features can improve performance through (i) *Scene Entities* (see Exp #2) or *Scene Activities* (see Exp #3):—either when only one type of scene element is fused with video representation, the R@1 score improved by a large margin of 1.4 (only scene entities) and 1.7 (only scene activ-

ities) compared to Baseline;—or, through *Scene Elements Aggregation* (see Exp #4), these features can be combined to enable an improvement over single feature utilization, with R@1 increased to 51.5 from 49.2 / 49.4. Furthermore, through (ii) *Captioning Head* (see Exp #5), better alignment between element-aware visual scene features and textual features can also be achieved, hinting that visual embeddings are enabled with finer-grained cross-modal features as R@1 increased from 51.5 to 52.1.

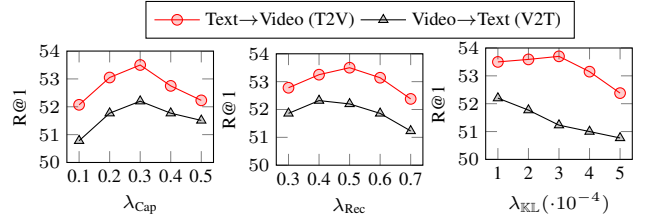


Figure 3. Hyperparameter sensitivity study on MSR-VTT.

**Effect of Textual Content Debias.** Table 4 shows the effect of the *Textual Content Debias* module. From Exp #5 and #7, we observe that the efficacy of the *Text Content Debias* and *Visual Scene Debias* improves R@1 from 52.1 to 53.5. This suggests that the *Textual Content Debias* module is complementary with *Visual Scene Debias* to improve performance.

**Effect of Textual Bias Features.** To evaluate the impact of bias on textual representations in retrieval tasks, we conduct a controlled analysis by fusing content and bias features using a weighted sum:  $\hat{\mathbf{t}}^{(i)} + \alpha \cdot \tilde{\mathbf{t}}^{(i)}$ , where  $\hat{\mathbf{t}}^{(i)}$  denotes the content embedding and  $\tilde{\mathbf{t}}^{(i)}$  the bias embedding. The scalar parameter  $\alpha$  modulates the degree of bias injected into the content representation. By varying  $\alpha$ , we systematically assess how retrieval performance degrades as bias intensity increases, thereby quantifying the trade-off between preserving semantic fidelity and suppressing bias-induced noise.

Quantitatively, in Figure 4, we illustrate the impact of varying  $\alpha$  on retrieval performance. As  $\alpha$  transitions from content-only to a mix of content and bias features, we observe that introducing more bias into the content increases noise during retrieval, which degrades performance. This demonstrates how the presence of bias disturbs the retrieval process.

As shown in Table 5, we further validate the importance of disentangling content features from bias features in the TVR task. Specifically, the use of content features  $\hat{\mathbf{t}}^{(i)}$  achieves significantly higher retrieval performance compared to the use of bias features  $\tilde{\mathbf{t}}^{(i)}$  across all recall metrics. When relying on  $\hat{\mathbf{t}}^{(i)}$  (content features), the model attains an R@1 of 53.5%, R@5 of 78.6%, and R@10 of 86.5%. In stark contrast, using  $\tilde{\mathbf{t}}^{(i)}$  (bias features) alone results in extremely poor performance, with R@1 dropping to 1.3%, R@5 to 10.2%, and R@10 to 18.9%. This substantial gap clearly illustrates that bias features, when isolated, fail to provide sufficient semantic grounding for accurate retrieval. Instead,

they appear to introduce noise that misleads the model away from the true video content, corroborating our earlier hypothesis that biases embedded in the linguistic patterns can harm retrieval accuracy if not properly handled. Ultimately, our analysis underscores that effective bias mitigation, *e.g.* using our proposed strategy, is essential for generalizable TVR.

Qualitatively, in Figure 5, we visualize the content and bias feature embeddings of 1,000 samples from the MSR-VTT test set using t-SNE [51]. The results show that our disentanglement process effectively separates content and bias components within the textual features. However, we also observe that some bias features remain partially entangled with the content representation. This highlights the inherent difficulty in completely disentangling bias information and suggests a promising direction for future investigation.

Additional ablation studies on **Effect of the Number of Scene Elements**, **Computational Cost**, and **Effect of Coefficient  $g$**  are included in the **Supplementary Material**, respectively.

Table 5. Ablation study between content features  $\hat{\mathbf{t}}$  or bias features  $\hat{\mathbf{b}}$  as textual features for T2V task on MSR-VTT.

Methods	R@1 $\uparrow$	R@5 $\uparrow$	R@10 $\uparrow$
using $\hat{\mathbf{t}}$ (content)	<b>53.5</b>	<b>78.6</b>	<b>86.5</b>
using $\hat{\mathbf{b}}$ (bias)	1.3	10.2	18.9

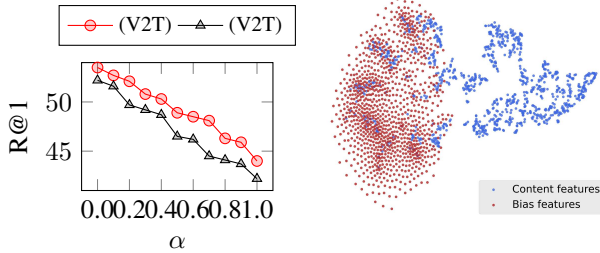


Figure 4. Effect of bias features on MSR-VTT.

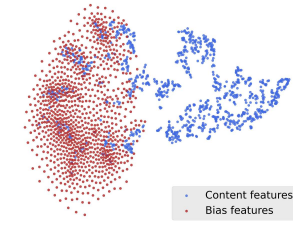


Figure 5. t-SNE [51] visualization between content and bias embeddings on MSR-VTT test set.

### 4.3. Qualitative Results

Figure 6 qualitatively demonstrates the performance of BiMa on MSR-VTT testset. We observe that BiMa is able to focus on relevant scene entities and scene activities, shown by the top three attention heatmaps per video, highlighting key elements in the scene. Further, BiMa can focus on small yet important actors and objects *e.g.*, the “alarm clock” in the 1<sup>st</sup> example and the “animal” in the 4<sup>th</sup> example. Next, BiMa also can focus on behaviors *e.g.*, “throwing” in the 4<sup>th</sup> example. This suggests that BiMa effectively integrates scene elements, which contributes to its improved retrieval accuracy over CLIP4Clip. In contrast, CLIP4Clip is unable to identify important scene elements and retrieves unrelated

results. In summary, the experimental results highlight the advantage of BiMa in associating visual content with textual descriptions, showing its enhanced performance in capturing nuanced visual features relevant to the query. Additional qualitative results are presented in the **Supplementary Material**.

## 5. Related Work

**Text-Video Retrieval.** TVR is a cross-modal retrieval task that aims to match videos with text descriptions [6, 7, 19, 21, 35, 49, 59]. Existing TVR methods typically leverage pre-trained VLMs like CLIP [40], BLIP [30] and adopt contrastive learning on pairs of samples to enhance their cross-modal representations across vision and language domains. Recent advancements, such as DiffusionRet [21], introduce multi-stage training mechanisms that use both discriminative and generative models to address challenges in out-of-domain retrieval tasks. In cases of ambiguous matching, where videos have multiple valid captions, uncertainty-based frameworks have emerged to handle this by learning a joint embedding space with probabilistic distance metrics. For example, UATVR [7] aligns cross-modal features as a distribution-matching procedure, while PAU [29] introduces semantic prototypes to capture ambiguous semantics within an uncertainty-based framework. Although our work also addresses data ambiguities, we distinguish between “bias” and “uncertainty” in terms of both definition and objective. We define “bias” as overlooked features stemming from coarse-grained data and annotator subjectivity, whereas “uncertainty” refers to the diversity within representations due to the variation of annotators. Our approach focuses on mitigating biases by recalibrating cross-modal features in the latent space and treating bias components as noise. In contrast, uncertainty-based methods attempt to model representation diversity by treating matched visual-linguistic representations as stochastic variables, and they do not directly alleviate visual-linguistic biases.

**Bias in Vision-Language Models.** Bias in VLMs has become a growing concern as these models, widely used in real-world applications, are often pre-trained on large internet-scale datasets. While this provides VLMs with extensive knowledge, it also makes them susceptible to inheriting biases present in the underlying data, such as cultural stereotypes, racial biases, and gender imbalances [2, 9, 32, 46]. For instance, CLIP and BLIP tend to amplify societal biases [55]. Recent literature explicitly categorizes these biases as representation biases—systematic deviations or skews within datasets, causing models to disproportionately rely on certain dataset-specific patterns rather than generalizable, task-relevant features [36, 45]. These biases typically manifest as concept bias (where models rely heavily on prominent visual concepts), temporal bias (where temporal aspects are inadequately represented), and textual bias (arising from



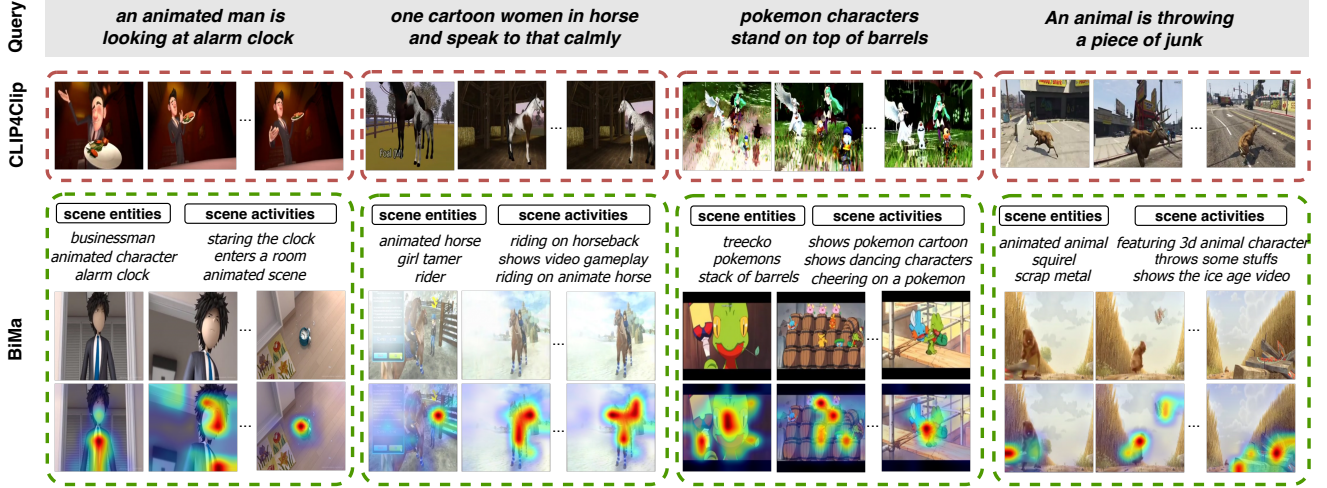


Figure 6. **TVR qualitative Results.** Videos in green boxes are true top-1 videos retrieved from BiMa, and in red boxes are false top-1 videos retrieved from CLIP4Clip. We also provide attention visualizations and the top 3 relevant scene elements for each video to show where BiMa is focused on.

subjective annotator interpretations or emotionally charged annotations) [45]. Additionally, recent empirical evaluations reveal that even modern datasets, designed with significant diversification efforts, still contain intrinsic dataset-specific biases, limiting models’ generalizability and robustness [36]. As VLMs become more prominent, addressing and mitigating these biases is critical for ensuring ethical and fair AI applications. For visual bias, existing approaches have relied on costly solutions such as simulators [26] or crowdsourcing [17, 39] to annotate visual features. These approaches are not scalable and lack universal applicability. Recent studies [53, 58] utilize scene factorization to eliminate biases in visual representation by focusing on relevant scene entities. However, many of these approaches rely heavily on computationally intensive object detectors, restricting their applicability to unseen scenarios. For textual bias, existing studies address biases in sentence embeddings by introducing training constraints [15] or directly modifying datasets [63]. Recent Autoencoder-based methods [5, 12, 22, 47] aim to detach the domain bias from textual representations. However, these methods typically rely on supervised learning using additional bias annotations, limiting their generalizability and scalability. To the best of our knowledge, BiMa represents a pioneering effort in systematically addressing these identified visual and textual representation biases in VLMs through the integration of scene element aggregation, visual attention redirection, and textual disentanglement. Crucially, our method is self-supervised and does not require additional human annotations, effectively addressing the limitations noted in prior studies [36, 45].

## 6. Conclusion

**Conclusion.** In this study, we addressed visual-linguistic bias challenges in the TVR task, drawing upon recent bias representation findings [36, 45] to address an unexplored area in the TVR literature. We proposed BiMa, a novel framework to mitigate biases in both visual and textual representations. Our proposed framework incorporates three modules— *Scene Element Construction*, *Visual Scene De-bias*, and *Textual Content De-bias*. Through extensive experiments and ablation studies across five major TVR benchmark datasets, we demonstrated the remarkable performance of our approach, surpassing existing SOTA TVR methods. Additionally, our BiMa exhibited remarkable performance in handling out-of-distribution retrieval problems showing the bias mitigation and generalization capabilities on unseen data variations.

**Limitation.** Although our taxonomy dictionary is constructed from diverse sources containing a comprehensive set of scene elements, some inherent biases may remain unmitigated. Addressing these challenges remains an avenue for future research.

**Broader Impacts.** BiMa advances generalize and robust TVR by mitigating dataset-specific biases through innovative, self-supervised techniques. By ensuring models focus on meaningful content rather than superficial features, this work not only boosts retrieval accuracy but also sets a new standard for developing generalized multimedia systems—paving the way for more flexible AI applications in diverse real-world scenarios.

Table .1. Effect of the number of scene elements on MSR-VTT.

$\kappa$	Scene Entities			Scene Activities		
	R@1 $\uparrow$	R@5 $\uparrow$	R@10 $\uparrow$	R@1 $\uparrow$	R@5 $\uparrow$	R@10 $\uparrow$
$\kappa = 10$	48.6	74.9	82.3	48.7	75.0	83.1
$\kappa = 15$	48.9	74.9	82.6	48.9	75.2	83.1
$\kappa = 20$	<b>49.2</b>	<b>75.3</b>	<b>83.0</b>	<b>49.4</b>	<b>75.7</b>	<b>83.4</b>
$\kappa = 25$	49.1	75.3	83.0	49.3	75.7	83.3
$\kappa = 30$	48.9	75.2	82.8	48.9	75.6	83.4

## A. Taxonomy Dictionary Details

To construct a comprehensive taxonomy dictionary that serves as a thesaurus of scene elements—encompassing both entities and activities expressed as noun and verb phrases—we adopt a dual-stage strategy involving large-scale language and multimodal models. Specifically, we employ the Large Language Model (LLM) QWEN2.5-7B [48, 60] to systematically extract phrasal expressions from video-text datasets, and the Large Multimodal Model (LMM) LLaVA-OV-7B [28] to enrich these expressions with visually plausible actions inferred from video content.

For phrasal extraction, we query the LLM QWEN2.5-7B using all captions available in existing TVR datasets with the prompt illustrated below. This prompt encourages the model to identify and group all possible *noun phrases* and *verb phrases* separately, while accounting for semantically equivalent variants:

### PROMPT

List all possible noun phrases and verb phrases in the given caption. Present the two lists separately, separated by a semicolon (;). Include alternative expressions for the same entity or action. For example, if the entity or action can be described in multiple ways, list them all. Ensure your output follows the format of the examples provided below.

**Caption:** In the heart of the kitchen, a man skillfully slices into a ripe mango, its golden flesh gleaming under the light.

**Verb phrases:** slicing a ripe mango; cutting into a ripe mango; gleaming under the light; shining in the light.

**Noun phrases:** the heart of the kitchen; a man; the man; a ripe mango; golden flesh; the light; the kitchen.

**Caption:** A woman sits by the fireplace, knitting a scarf as the flames crackle warmly in the background.

**Verb phrases:** sitting by the fireplace; sitting near the fireplace; knitting a scarf; knitting a piece of cloth; crackling in the background; burning in the background.

**Noun phrases:** a woman; the woman; the fireplace; a scarf; the flames; the fire; the background.

To complement this text-based extraction, we employ the LMM LLaVA-OV-7B to analyze the raw visual content of videos in the same datasets. The model is prompted to generate a list of plausible short narrations in the form of verb-noun phrases (e.g., “slicing mango”), effectively capturing fine-grained, visually grounded actions that may not be explicitly mentioned in captions:

Table .2. **Computational costs** of BiMa w.r.t. different  $\kappa$  on MSR-VTT with a gallery size of 1,000 candidate videos and 1,000 text queries. The best and second best are **bold** and underlined.

Methods	Computational Cost		Performance R@1 $\uparrow$
	Inference Time (s) $\downarrow$	Memory (GB) $\downarrow$	
CLIP4Clip (baseline)	<b>31.12</b>	<b>4.1</b>	45.7
BiMa ( $\kappa = 10$ )	36.25	<u>4.3</u>	52.9
BiMa ( $\kappa = 15$ )	36.33	<u>4.3</u>	53.2
BiMa ( $\kappa = 20$ )	<u>36.40</u>	<u>4.3</u>	<b>53.5</b>
BiMa ( $\kappa = 25$ )	36.49	<u>4.3</u>	53.3
BiMa ( $\kappa = 30$ )	36.52	<u>4.3</u>	53.1

Table .3. Ablation study on dataset combination of taxonomy dictionary.

Dataset Source					T2V		
MSR-VTT	MSVD	LSMDC	ActivityNet	DiDeMo	R@1 $\uparrow$	R@5 $\uparrow$	R@10 $\uparrow$
✓	✗	✗	✗	✗	49.7	75.7	83.8
✓	✓	✗	✗	✗	49.9	75.9	84.2
✓	✓	✓	✗	✗	50.4	76.1	84.6
✓	✓	✓	✓	✗	51.0	76.4	84.6
✓	✓	✓	✓	✓	<b>51.5</b>	<b>76.6</b>	<b>84.8</b>

Table .4. Effectiveness of coefficient  $g$  on Scene Elements Aggregation module on MSR-VTT.

Method	R@1 $\uparrow$	R@5 $\uparrow$	R@10 $\uparrow$
without $g$	49.9	76.0	84.1
with $g$	<b>51.5</b>	<b>76.6</b>	<b>84.8</b>

### PROMPT

List all possible actions that could take place in the scene of the given video. Write each action as a short narration (a verb with a noun), separated by a semicolon (;). Follow the structure shown in the examples below.

**Video:** {video #}

**Narration:** Slicing mango; Holding knife; Cutting mango; Placing seed; Wiping counter; Dropping pieces; Gripping mango; Resting knife; Smelling mango; Gathering chunks.

**Video:** {video #}

**Narration:** Knitting scarf; Holding needles; Looping yarn; Adjusting thread; Pulling stitch; Resting hands; Dropping yarn; Smelling smoke; Listening to flames; Rubbing hands; Folding scarf; Gathering wool; Staring at fire; Sitting still; Tapping needle.

After collecting these phrasal outputs, we apply deduplication to retain only unique noun and verb phrases. This process results in a diverse and comprehensive lexicon of scene elements, which we visualize as word clouds in Fig. B.1, with each cloud representing a different dataset. As shown in Fig. B.2, our method successfully extracts a total of 86,159 distinct noun phrases and 141,981 distinct verb phrases across five large-scale TVR benchmarks: MSR-VTT, MSVD, LSMDC, ActivityNet Captions, and DiDeMo.

For each dataset, we also provide examples of it in Table D.5 to demonstrate the different variations of textual annotations, hinting at the textual biases that can be encoun-

tered.

## B. Scene Elements Details

The abundance of noun and verb phrases in video-text annotations introduces potential sources of inherent bias, as different textual descriptions for the same visual content can vary significantly in focus, vocabulary, and granularity. Consequently, models trained on such data may inadvertently overfit to specific linguistic patterns, leading to sub-optimal generalization. To address this, we construct a large-scale vocabulary of scene elements—spanning entities and actions—from a diverse collection of datasets to dilute such biases during training.

Our core hypothesis is that smaller or domain-specific dictionaries are more prone to encoding biases, whereas larger and more diverse vocabularies help reduce representational skew by incorporating a broader spectrum of semantic features. Empirical results from our ablation study (Table 4 - Main paper) validate this hypothesis: models utilizing Scene Elements consistently outperform those without, highlighting their effectiveness in mitigating bias.

To build this robust vocabulary, we aggregate scene elements from five large-scale TVR benchmarks: MSR-VTT, MSVD, LSMDC, ActivityNet Captions, and DiDeMo. As shown in Table .3, increasing the number of datasets used to construct the dictionary yields consistent performance gains, further underscoring the importance of diverse and fine-grained video descriptions for reducing bias.

To further improve the quality and robustness of the taxonomy, we advocate for extending it to include additional datasets from varied domains. Furthermore, we propose exploring an open-vocabulary setting in which the dictionary is dynamically expanded during training to accommodate emerging or domain-specific scene elements. We leave the design of such adaptive and scalable vocabularies as a promising direction for future research.

Further, we observe that the number of verb phrases is approximately two times more than the number of noun phrases. This is because an actor can perform various activities, and annotators use different tenses and synonyms to describe activity(s), actor(s) in a video can engage in a list of behaviors. Moreover, given that the number of verb phrases is more than the number of noun phrases, the verb phrases may inject more bias into TVR frameworks than noun phrases. Consequently, if we can mitigate biases that come from verb phrases, we may achieve better accuracy than mitigating biases that come from noun phrases. This aligns with the ablation study result (see Table .1). We observe that when solely integrating scene activities (i.e., verb phrases), we attain superior accuracy (with an increase of over 2% on R@1 metrics) compared to when only integrating scene entities (i.e., noun phrases).

## C. Additional Ablation Studies

To further illustrate the capabilities of our BiMa, we conduct additional quantitative analyses as follows:

- Table .1 illustrates the effectiveness of the number of scene elements used.
- Table .2 shows the efficiency of our method versus the baseline, across different number of scene elements.
- Table .4 illustrates the effectiveness of the coefficient  $g$ .

**Effect of the Number of Scene Elements.** The number of scene elements  $\kappa$  controls how many scene elements are fused into the video representation. In Table .1, the overall performance improves and then decreases. We observe that a small number of scene elements may limit the effect of the Visual Scene Debias module to focus on fine-grained information in the visual scene. However, a larger number of scene elements reduces the discriminability of the video representation. We achieve the best performance with  $\kappa = 20$ .

**Computational Cost.** In practical scenarios, the taxonomy dictionary’s integration is computationally efficient, as it matches each video with scene elements to find the top- $\kappa$  relevant scene elements only once. Table .2 presents comparison on computational cost and performance, detailing both inference time and memory usage. We observe that BiMa achieves higher accuracy than CLIP4Clip while only incurring a slight increase in inference time and maintaining comparable memory consumption. Additionally, as  $\kappa$  increases, the impact on BiMa’s computational cost becomes minimal. This experiment demonstrates that BiMa is computationally efficient and balances accuracy with resource usage effectively. For enhanced efficiency, the final fusion feature vectors between each video and top- $\kappa$  relevant scene elements can be directly indexed into the target database to reduce the fusion step during inference.

**Effect of the coefficient  $g$ .** As depicted in Table .4, we show that coefficient  $g$  can amplify the discriminative characteristic of each original feature by facilitating a seamless embedding aggregation process by acting as the association between each feature token and its most closely relevant token from the other feature tokens. After integrate the coefficient  $g$  into the *Scene Element Aggregation* module (in the main paper), the performance increase by 0.5% w.r.t R@1.

## D. Additional Qualitative Visualizations

To further illustrate the debias capabilities of our BiMa, we conduct additional qualitative comparisons between our BiMa and CLIP4Clip as follows:

- Figs. B.1 and B.2 respectively show the word clouds and statistics on dataset-specific scene elements that we extracted based on our taxonomy dictionary.
- Figs. D.3, D.4, and D.5 show the visual attention heatmaps generated by our BiMa model in comparison

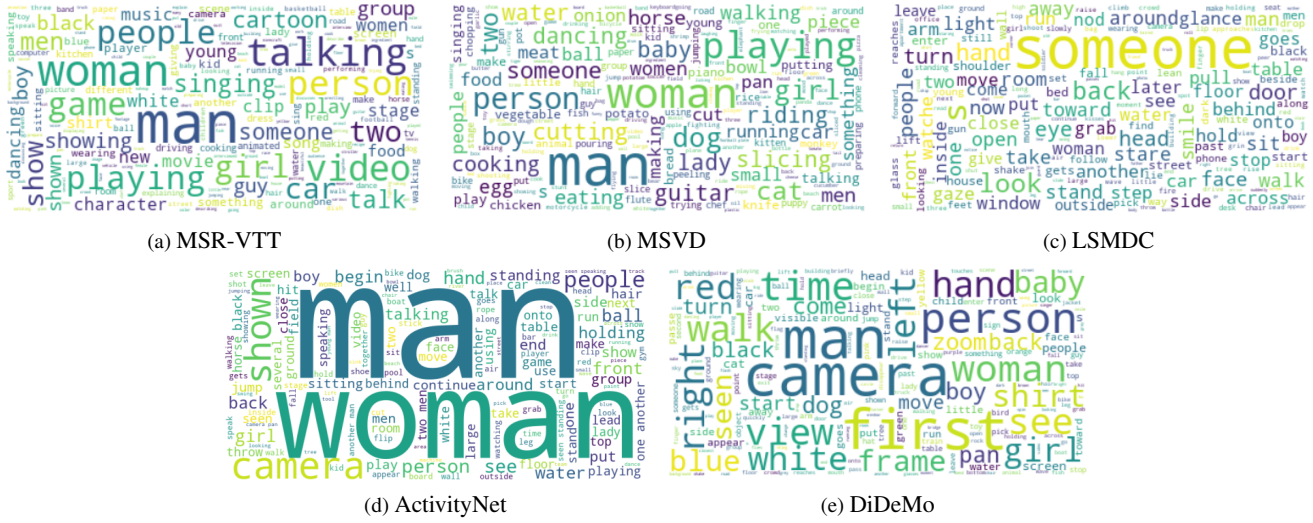


Figure B.1. Word clouds of textual descriptions in different datasets.

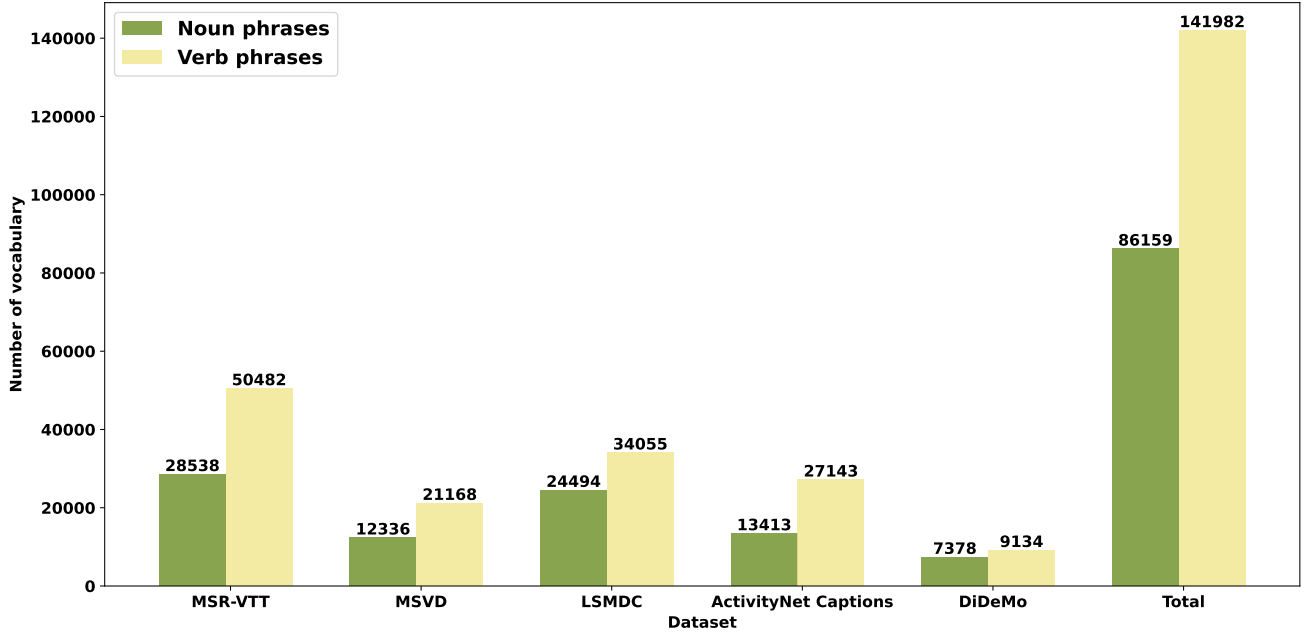


Figure B.2. Taxonomy Dictionary.

with CLIP4Clip on the T2V task.

- Figs. D.6 and D.7 illustrate the robustness and efficacy of the proposed BiMa.
- Fig. D.8 demonstrates how the same video can be retrieved using different input text queries.

**Attention Map Comparison** To gain deeper insights into the bias mitigation capability of our BiMa, we conduct the attention map visualizations generated using gradCAM [42] between our BiMa and the baseline model CLIP4Clip, as illustrated in Figs. D.3, D.4, and D.5. The attention maps re-

veal that our proposed BiMa effectively captures the essence of scene elements in the video. As shown in the second frame of Figs. D.4 and D.5, we observe that BiMa can focus on small-size actors (e.g., the singer and the horse) and disregard the distractive environment. Further, the attention map completely matches the top-3 scene entities, which also can be employed as explainability in further research. These results demonstrate BiMa ability to capture crucial scene elements present in the video, thereby enabling successful video retrieval.



Dataset	Examples
MSR-VTT (~43 characters in a text)	1) A bulldozer removes dirt 2) An infomercial with a pharmaceutical company talking about an epilepsy drug pending approval from the FDA 3) Extreme violence scenes with people fighting with each other 4) A woman is in front of a whiteboard talking about the numbers written on it 5) A man is playing an instrument
MSVD (~31 characters in a text)	1) A lady is pouring raw strawberry juice into a bowl 2) A man is slicing the crust into a potato 3) A man lifts three sunflowers 4) A man is putting a pan into an oven 5) A boy rides around in circles on a tricycle
LSMDC (~46 characters in a text)	1) The dish is covered in saffron and spices. 2) He slaps SOMEONE again. 3) He and SOMEONE join forces to grab the cube, which's connected with several more wire. 4) In the race, a rider falls. 5) SOMEONE dashes to a clothes closet and ducks inside. The cup spins across the floor.
ActivityNet (~67 characters in a text)	1) A man is seen speaking to the camera and pans out into more men standing behind him. 2) A woman is seen kneeling down next to a man. 3) Several people are shown doing long boarding stunts in the parking lots of a college. 4) People are sitting inside of a raft going over large bumps in the water. 5) Several shots are shown of a man speaking to groups of people and leads into people wearing wet suits and walking.
DiDeMo (~147 characters in a text)	1) First time we see the dancers go down on one leg the men hit the ground with their sticks. They first start crouching and hitting the ground with the sticks 2) When the man puts his head down the guitar player is looking up. The guitarist is looking straight up. A man plays the guitar while looking up. The guitarist is looking straight up as he plays. 3) Red phone booth is visible a red phone booth is in the scene. A person walks in the middle of the camera. A red phone booth can be seen a red telephone booth is on the sidewalk. 4) The camera moves back to the left to the tree. White square exits frame left the camera pans back the way it came. Square area lines with stones comes into view the fence comes into view. 5) Fog moves in toward the ice skater. a woman spins around several times very fast. A woman pirouettes as she comes near the camera. Woman spins more than 5 times in a row.

Table D.5. Five random examples of text descriptions in different datasets. For each dataset, we also report the median length of a text in that dataset on the left column.

**Text-to-Video Retrieval** In Figs. D.6 and D.7, we provide Text-to-video (T2V) comparisons between our BiMa and the baseline model CLIP4Clip. Remarkably, our method consistently retrieves the ground truth video as the 1st rank video. These results demonstrate that our method can align video and text effectively.

Additionally, we present additional retrieval examples in Fig. D.8, utilizing various textual queries of the same ground truth video. This figure serves as a comparison between our BiMa and the baseline model CLIP4Clip. We observe that our proposed BiMa consistently retrieves the ground truth video across different textual queries, while CLIP4Clip often retrieves incorrect results.

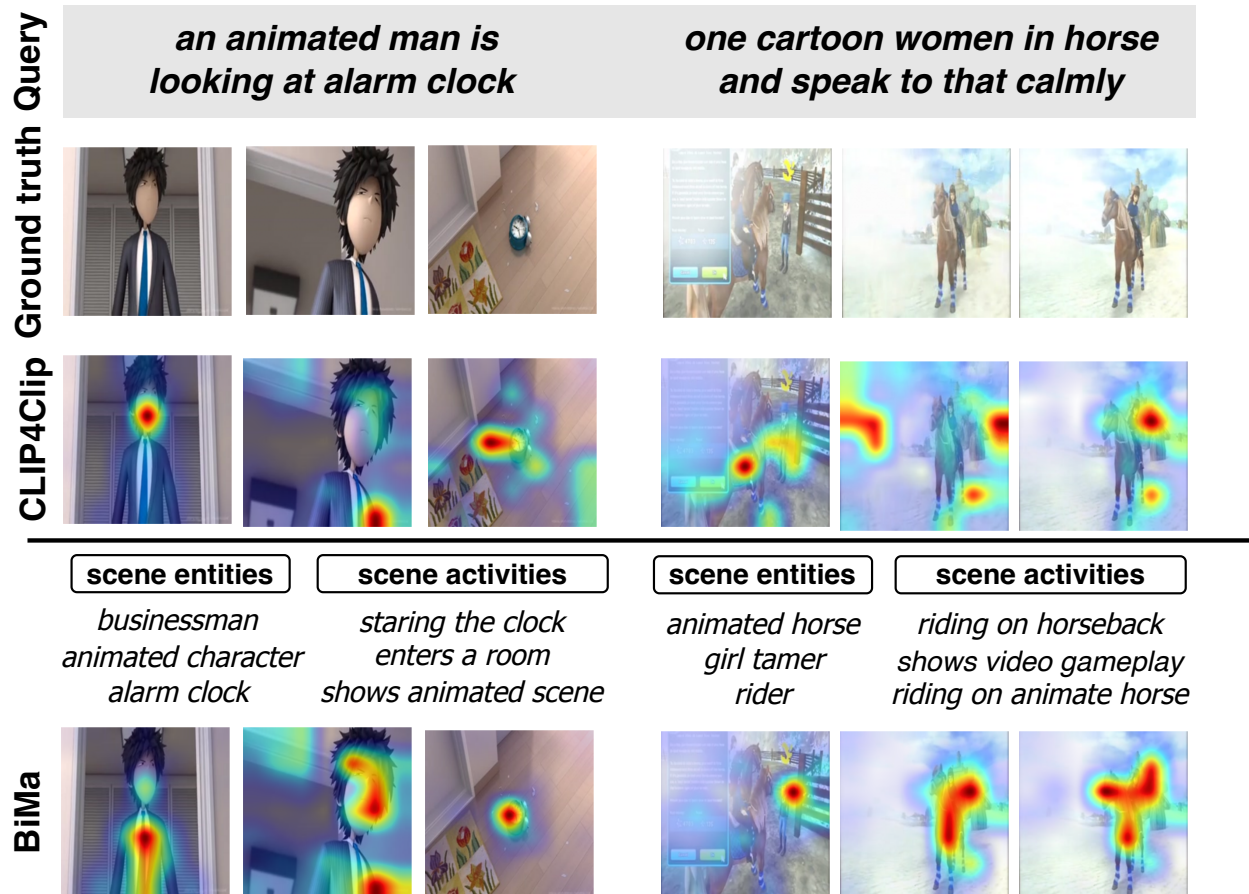


Figure D.3. **Attention Map Results.** From top-to-bottom: Textual query description, ground truth video, CLIP4Clip’s attention map and BiMa’s attention map.

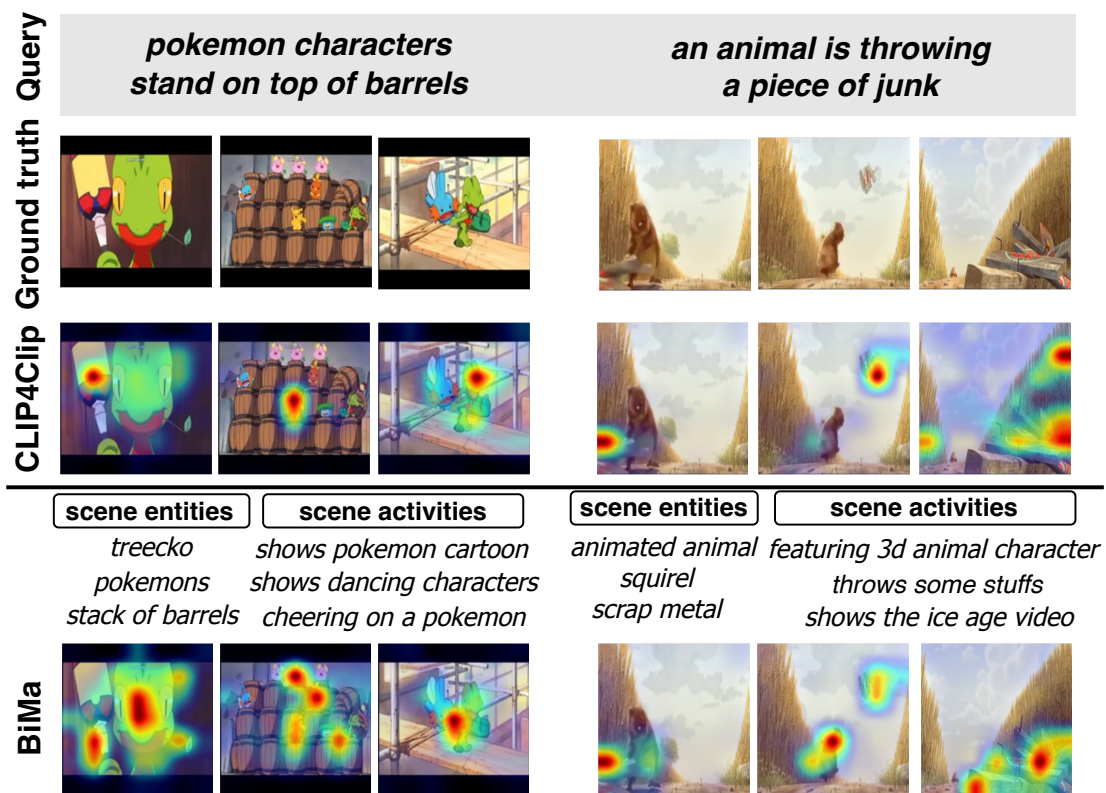


Figure D.4. **Attention Map Results.** From top-to-bottom: Textual query description, ground truth video, CLIP4Clip’s attention map and BiMa’s attention map.

CLIP4Clip Ground truth Query

*a man is singing on stage to a huge audience, he is holding microphone*

*person is recording brown horse which is having fun*



**scene entities**

**scene activities**

*singers  
vocalists  
show performances*  
*playing the voice tv show  
performs singing competition  
announcing the singer*

**scene entities**

**scene activities**

*quarter horse  
rodeo  
galloping horse*  
*featuring horse tricks  
filming a brown horse  
playing stampede*

BiMa



Figure D.5. **Attention Map Results.** From top-to-bottom: Textual query description, ground truth video, CLIP4Clip's attention map and BiMa's attention map.





Figure D.6. **Text-to-video Results.** On the left are BiMa’s retrieval results and on the right are CLIP4Clip’s retrieval results. Ground truth videos are highlighted in the green box. These results demonstrate that our method can align the correlation between text and video effectively.

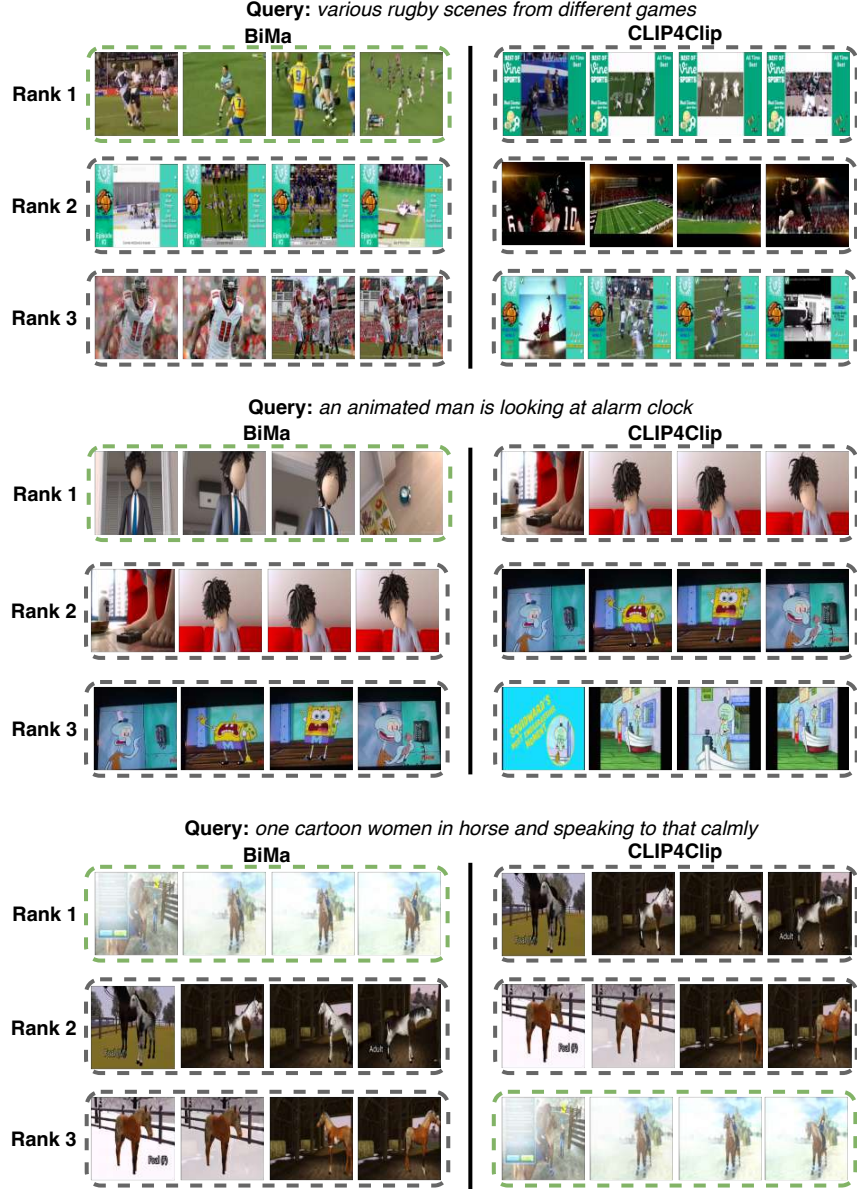


Figure D.7. **Text-to-video Results.** On the left are BiMa’s retrieval results and on the right are CLIP4Clip’s retrieval results. Ground truth videos are highlighted in the green box. These results demonstrate that our method can align the correlation between text and video effectively.



Figure D.8. **Different Queries Text-to-video Results.** We show retrieval results on two different queries of the same ground truth video. On the left are BiMa’s retrieval results and on the right are CLIP4Clip’s retrieval results. Ground truth videos are highlighted in the green box. These results demonstrate that our method can retrieve consistently despite different query content.



## References

- [1] Max Bain, Arsha Nagrani, Gül Varol, and Andrew Zisserman. Frozen in time: A joint video and image encoder for end-to-end retrieval. In *IEEE/CVF International Conference on Computer Vision (ICCV)*, pages 1708–1718, 2021. 6
- [2] Tolga Bolukbasi, Kai-Wei Chang, James Y Zou, Venkatesh Saligrama, and Adam T Kalai. Man is to computer programmer as woman is to homemaker? debiasing word embeddings. *Annual Conference on Neural Information Processing Systems (NeurIPS)*, pages 4349–4357, 2016. 8
- [3] David L. Chen and William B. Dolan. Collecting highly parallel data for paraphrase evaluation. In *Annual Meeting of the Association for Computational Linguistics: Human Language Technologies (ACL)*, pages 190–200, 2011. 1, 5
- [4] Shizhe Chen, Yida Zhao, Qin Jin, and Qi Wu. Fine-grained video-text retrieval with hierarchical graph reasoning. In *IEEE/CVF Conference on Computer Vision and Pattern Recognition (CVPR)*, pages 10635–10644, 2020. 7
- [5] Tianlang Chen, Zhongping Zhang, Quanzeng You, Chen Fang, Zhaowen Wang, Hailin Jin, and Jiebo Luo. “factual” or “emotional”: Stylized image captioning with adaptive learning and attention. In *European Conference on Computer Vision (ECCV)*, pages 527–543, 2018. 9
- [6] Yizhen Chen, Jie Wang, Lijian Lin, Zhongang Qi, Jin Ma, and Ying Shan. Tagging before alignment: Integrating multi-modal tags for video-text retrieval. In *AAAI Conference on Artificial Intelligence (AAAI)*, pages 396–404, 2023. 6, 8
- [7] Bo Fang, Wenhao Wu, Chang Liu, Yu Zhou, Yuxin Song, Weiping Wang, Xiangbo Shu, Xiangyang Ji, and Jingdong Wang. UATVR: uncertainty-adaptive text-video retrieval. In *IEEE/CVF International Conference on Computer Vision (ICCV)*, pages 13677–13687, 2023. 6, 8
- [8] Valentin Gabeur, Chen Sun, Karteek Alahari, and Cordelia Schmid. Multi-modal transformer for video retrieval. In *European Conference on Computer Vision (ECCV)*, pages 214–229, 2020. 5
- [9] Nikhil Garg, Londa Schiebinger, Dan Jurafsky, and James Zou. Word embeddings quantify 100 years of gender and ethnic stereotypes. *Proceedings of the National Academy of Sciences*, 115(16):3635–3644, 2018. 8
- [10] Satya Krishna Gorti, Noël Vouitsis, Junwei Ma, Keyvan Golestan, Maksims Volkovs, Animesh Garg, and Guangwei Yu. X-pool: Cross-modal language-video attention for text-video retrieval. In *IEEE/CVF Conference on Computer Vision and Pattern Recognition (CVPR)*, pages 4996–5005, 2022. 6
- [11] Priya Goyal, Piotr Dollár, Ross B. Girshick, Pieter Noordhuis, Lukasz Wesolowski, Aapo Kyrola, Andrew Tulloch, Yangqing Jia, and Kaiming He. Accurate, large minibatch SGD: training imagenet in 1 hour. *arXiv preprint arXiv:1706.02677*, 2017. 5
- [12] Longteng Guo, Jing Liu, Peng Yao, Jiangwei Li, and Hanqing Lu. Mscap: Multi-style image captioning with unpaired stylized text. In *IEEE/CVF Conference on Computer Vision and Pattern Recognition (CVPR)*, pages 4204–4213, 2019. 9
- [13] Lisa Anne Hendricks, Oliver Wang, Eli Shechtman, Josef Sivic, Trevor Darrell, and Bryan C. Russell. Localizing moments in video with natural language. In *IEEE/CVF International Conference on Computer Vision (ICCV)*, pages 5804–5813, 2017. 1, 5
- [14] Irina Higgins, Loïc Matthey, Arka Pal, Christopher P. Burgess, Xavier Glorot, Matthew M. Botvinick, Shakir Mohamed, and Alexander Lerchner. beta-VAE: Learning basic visual concepts with a constrained variational framework. In *International Conference on Learning Representations (ICLR)*, 2017. 4
- [15] Po-Sen Huang, Huan Zhang, Ray Jiang, Robert Stanforth, Johannes Welbl, Jack Rae, Vishal Maini, Dani Yogatama, and Pushmeet Kohli. Reducing sentiment bias in language models via counterfactual evaluation. In *Findings of Conference on Empirical Methods in Natural Language Processing (EMLP)*, pages 65–83, 2020. 9
- [16] Chan Hur, Jeong hun Hong, Dong hun Lee, Dabin Kang, Semin Myeong, Sang hyo Park, and Hyeyoung Park. Narrating the video: Boosting text-video retrieval via comprehensive utilization of frame-level captions. In *IEEE/CVF Conference on Computer Vision and Pattern Recognition (CVPR)*, 2025. 1, 6, 7
- [17] Badr Youbi Idrissi, Diane Bouchacourt, Randall Balestriero, Ivan Evtimov, Caner Hazirbas, Nicolas Ballas, Pascal Vincent, Michal Drozdal, David Lopez-Paz, and Mark Ibrahim. Imagenet-x: Understanding model mistakes with factor of variation annotations. In *International Conference on Learning Representation (ICLR)*, 2023. 9
- [18] Peng Jin, Jinfa Huang, Fenglin Liu, Xian Wu, Shen Ge, Guoli Song, David A. Clifton, and Jie Chen. Expectation-maximization contrastive learning for compact video-and-language representations. In *Annual Conference on Neural Information Processing Systems (NeurIPS)*, pages 30291–30306, 2022. 6
- [19] Peng Jin, Jinfa Huang, Pengfei Xiong, Shangxuan Tian, Chang Liu, Xiangyang Ji, Li Yuan, and Jie Chen. Video-text as game players: Hierarchical banzhaf interaction for cross-modal representation learning. In *IEEE/CVF Conference on Computer Vision and Pattern Recognition (CVPR)*, pages 2472–2482, 2023. 6, 8
- [20] Peng Jin, Hao Li, Zesen Cheng, Jinfa Huang, Zhennan Wang, Li Yuan, Chang Liu, and Jie Chen. Text-video retrieval with disentangled conceptualization and set-to-set alignment. In *International Joint Conference on Artificial Intelligence (IJCAI)*, pages 938–946, 2023. 6
- [21] Peng Jin, Hao Li, Zesen Cheng, Kehan Li, Xiangyang Ji, Chang Liu, Li Yuan, and Jie Chen. DiffusionRet: Generative text-video retrieval with diffusion model. In *IEEE/CVF International Conference on Computer Vision (ICCV)*, pages 2470–2481, 2023. 6, 8
- [22] Vineet John, Lili Mou, Hareesh Bahuleyan, and Olga Vechtomova. Disentangled representation learning for non-parallel text style transfer. In *Annual Meeting of the Association for Computational Linguistics: Human Language Technologies (ACL)*, pages 424–434, 2019. 9
- [23] Diederik P. Kingma and Jimmy Ba. Adam: A method for stochastic optimization. In *International Conference on Learning Representation (ICLR)*, 2015. 5
- [24] Diederik P. Kingma and Max Welling. Auto-encoding variational Bayes. In *International Conference on Learning Representation (ICLR)*, 2014. 4
- [25] Ranjay Krishna, Kenji Hata, Frederic Ren, Li Fei-Fei, and Juan Carlos Niebles. Dense-captioning events in videos. In *IEEE/CVF International Conference on Computer Vision (ICCV)*, pages 706–715, 2017. 1, 5
- [26] Guillaume Leclerc, Hadi Salman, Andrew Ilyas, Sai Vemprala, Logan Engstrom, Vibhav Vineet, Kai Xiao, Pengchuan Zhang, Shibani Santurkar, Greg Yang, et al. 3db: A framework for debugging computer vision models. In *Annual Conference on Neural Information Processing Systems (NeurIPS)*, pages 8498–8511, 2022. 9
- [27] Jie Lei, Linjie Li, Luwei Zhou, Zhe Gan, Tamara L. Berg, Mohit Bansal, and Jingjing Liu. Less is more: Clipbert for video-and-language learning via sparse sampling. In *IEEE/CVF International Conference on Computer Vision and Pattern Recognition (CVPR)*, pages 7331–7341, 2021. 6
- [28] Bo Li, Yuanhan Zhang, Dong Guo, Renrui Zhang, Feng Li, Hao Zhang, Kaichen Zhang, Yanwei Li, Ziwei Liu, and Chunyuan Li. Llava-onevision: Easy visual task transfer. *arXiv preprint arXiv:2408.03326*, 2024. 1
- [29] Hao Li, Jingkuan Song, Lianli Gao, Xiaosu Zhu, and Hengtao Shen. Prototype-based aleatoric uncertainty quantification for cross-modal retrieval. In *Annual Conference on Neural Information Processing Systems (NeurIPS)*, pages 24564–2458, 2023. 8
- [30] Junnan Li, Dongxu Li, Caiming Xiong, and Steven Hoi. Blip: Bootstrapping language-image pre-training for unified vision-language understanding and generation. In *International Conference on Machine Learning (ICML)*, pages 12888–12900, 2022. 1, 8



- [31] Manling Li, Ruochen Xu, Shuohang Wang, Luowei Zhou, Xudong Lin, Chenguang Zhu, Michael Zeng, Heng Ji, and Shih-Fu Chang. Clip-event: Connecting text and images with event structures. In *IEEE/CVF Conference on Computer Vision and Pattern Recognition (CVPR)*, pages 16420–16429, 2022. 1
- [32] Paul Pu Liang, Irene Mengze Li, Emily Zheng, Yao Chong Lim, Ruslan Salakhutdinov, and Louis-Philippe Morency. Towards debiasing sentence representations. In *Annual Meeting of the Association for Computational Linguistics: Human Language Technologies (ACL)*, 2020. 8
- [33] Chengzhi Lin, Ancong Wu, Junwei Liang, Jun Zhang, Wenhang Ge, Wei-Shi Zheng, and Chunhua Shen. Text-adaptive multiple visual prototype matching for video-text retrieval. *Annual Conference on Neural Information Processing Systems (NeurIPS)*, pages 38655–38666, 2022. 6
- [34] Fan Liu, Huilin Chen, Zhiyong Cheng, Anan Liu, Liqiang Nie, and Mohan Kankanhalli. Disentangled multimodal representation learning for recommendation. *IEEE Transactions on Multimedia*, 25:7149–7159, 2022. 5
- [35] Yuqi Liu, Pengfei Xiong, Luhui Xu, Shengming Cao, and Qin Jin. Ts2-net: Token shift and selection transformer for text-video retrieval. In *European Conference on Computer Vision (ECCV)*, pages 319–335, 2022. 6, 8
- [36] Zhuang Liu and Kaiming He. A decade’s battle on dataset bias: Are we there yet? In *ICLR*, 2025. 1, 2, 8, 9
- [37] Huaishao Luo, Lei Ji, Ming Zhong, Yang Chen, Wen Lei, Nan Duan, and Tianrui Li. Clip4clip: An empirical study of clip for end to end video clip retrieval and captioning. *Neurocomputing*, 508:293–304, 2022. 5, 6
- [38] Mandela Patrick, Po-Yao Huang, Yuki Markus Asano, Florian Metze, Alexander G. Hauptmann, João F. Henriques, and Andrea Vedaldi. Support-set bottlenecks for video-text representation learning. In *International Conference on Learning Representations (ICLR)*, 2021. 6
- [39] Gregory Plumb, Marco Túlio Ribeiro, and Ameet Talwalkar. Finding and fixing spurious patterns with explanations. *Transactions on Machine Learning Research*, 2022. 9
- [40] Alec Radford, Jong Wook Kim, Chris Hallacy, Aditya Ramesh, Gabriel Goh, Sandhini Agarwal, Girish Sastry, Amanda Askell, Pamela Mishkin, Jack Clark, et al. Learning transferable visual models from natural language supervision. In *International Conference on Machine Learning (ICML)*, pages 8748–8763, 2021. 1, 8
- [41] Anna Rohrbach, Atousa Torabi, Marcus Rohrbach, Niket Tandon, Christopher Pal, Hugo Larochelle, Aaron Courville, and Bernt Schiele. Movie description. *International Journal of Computer Vision*, 123: 94–120, 2017. 1, 5
- [42] Ramprasaath R Selvaraju, Michael Cogswell, Abhishek Das, Ramakrishna Vedantam, Devi Parikh, and Dhruv Batra. Grad-cam: Visual explanations from deep networks via gradient-based localization. In *IEEE/CVF International Conference on Computer Vision (ICCV)*, pages 618–626, 2017. 3
- [43] Leqi Shen, Tianxiang Hao, Tao He, Sicheng Zhao, Yifeng Zhang, pengzhang liu, Yongjun Bao, and Guiguang Ding. Tempme: Video temporal token merging for efficient text-video retrieval. In *ICLR*, 2025. 6
- [44] Nina Shvetsova, Anna Kukleva, Bernt Schiele, and Hilde Kuehne. In-style: Bridging text and uncurated videos with style transfer for text-video retrieval. In *IEEE/CVF Conference on Computer Vision and Pattern Recognition (CVPR)*, pages 21981–21992, 2023. 1, 6
- [45] Nina Shvetsova, Arsha Nagrani, Bernt Schiele, Hilde Kuehne, and Christian Rupprecht. Unbiasing through textual descriptions: Mitigating representation bias in video benchmarks. In *IEEE/CVF Conference on Computer Vision and Pattern Recognition (CVPR)*, 2025. 1, 2, 8, 9
- [46] Tony Sun, Andrew Gaut, Shirlyn Tang, Yuxin Huang, Mai ElSherief, Jieyu Zhao, Diba Mirza, Elizabeth M. Belding, Kai-Wei Chang, and William Yang Wang. Mitigating gender bias in natural language processing: Literature review. In *Annual Meeting of the Association for Computational Linguistics: Human Language Technologies (ACL)*, pages 1630–1640, 2019. 8
- [47] Yutong Tan, Zheng Lin, Peng Fu, Mingyu Zheng, Lanrui Wang, Yanan Cao, and Weiping Wang. Detach and attach: Stylized image captioning without paired stylized dataset. In *ACM International Conference on Multimedia (MM)*, pages 4733–4741, 2022. 9
- [48] Qwen Team. Qwen2.5: A party of foundation models, 2024. 1
- [49] Kaibin Tian, Ruixiang Zhao, Zijie Xin, Bangxiang Lan, and Xirong Li. Holistic features are almost sufficient for text-to-video retrieval. In *IEEE/CVF Conference on Computer Vision and Pattern Recognition (CVPR)*, pages 17138–17147, 2024. 1, 6, 8
- [50] Aäron van den Oord, Yazhe Li, and Oriol Vinyals. Representation learning with contrastive predictive coding. *arXiv preprint arXiv:1807.03748*, 2018. 5
- [51] Laurens van der Maaten and Geoffrey Hinton. Visualizing data using t-SNE. *Journal of Machine Learning Research*, 9:2579–2605, 2008. 8
- [52] Ashish Vaswani, Noam Shazeer, Niki Parmar, Jakob Uszkoreit, Llion Jones, Aidan N. Gomez, Lukasz Kaiser, and Illia Polosukhin. Attention is all you need. In *Annual Conference on Neural Information Processing Systems (NeurIPS)*, pages 5998–6008, 2017. 4
- [53] Khoa Vo, Sang Truong, Kashu Yamazaki, Bhiksha Raj, Minh-Triet Tran, and Ngan Le. Aoe-net: Entities interactions modeling with adaptive attention mechanism for temporal action proposals generation. *International Journal of Computer Vision*, 131(1):302–323, 2023. 9
- [54] Jiamian Wang, Pichao Wang, Dongfang Liu, Qiang Guan, Sohail A. Dianat, Majid Rabbani, Raghuveer Rao, and Zhiqiang Tao. Diffusion-inspired truncated sampler for text-video retrieval. In *Advances in Neural Information Processing Systems 38: Annual Conference on Neural Information Processing Systems 2024 NeurIPS 2024*, 2024. 5, 6
- [55] Zeyu Wang, Klint Qinami, Ioannis Christos Karakozis, Kyle Genova, Prem Nair, Kenji Hata, and Olga Russakovsky. Towards fairness in visual recognition: Effective strategies for bias mitigation. In *IEEE/CVF Conference on Computer Vision and Pattern Recognition (CVPR)*, pages 8916–8925, 2020. 8
- [56] Jian Xiao, Zhenzhen Hu, Jia Li, and Richang Hong. Text proxy: Decomposing retrieval from a 1-to-n relationship into n 1-to-1 relationships for text-video retrieval. In *Proceedings of the AAAI Conference on Artificial Intelligence*, 2025. 1, 5, 6
- [57] Jun Xu, Tao Mei, Ting Yao, and Yong Rui. Msr-vtt: A large video description dataset for bridging video and language. In *IEEE/CVF Conference on Computer Vision and Pattern Recognition (CVPR)*, pages 5288–5296, 2016. 1, 5
- [58] Kashu Yamazaki, Khoa Vo, Quang Sang Truong, Bhiksha Raj, and Ngan Le. Vltint: visual-linguistic transformer-in-transformer for coherent video paragraph captioning. In *AAAI Conference on Artificial Intelligence (AAAI)*, pages 3081–3090, 2023. 9
- [59] Rui Yan, Mike Zheng Shou, Yixiao Ge, Jinpeng Wang, Xudong Lin, Guanyu Cai, and Jinhui Tang. Video-text pre-training with learned regions for retrieval. In *AAAI Conference on Artificial Intelligence (AAAI)*, pages 3100–3108, 2023. 6, 8
- [60] An Yang, Baosong Yang, Binyuan Hui, Bo Zheng, Bowen Yu, Chang Zhou, Chengpeng Li, Chengyuan Li, Dayiheng Liu, Fei Huang, Guanting Dong, Haoran Wei, Huan Lin, Jialong Tang, Jialin Wang, Jian Yang, Jianhong Tu, Jianwei Zhang, Jianxin Ma, Jin Xu, Jingren Zhou, Jinze Bai, Jinzheng He, Junyang Lin, Kai Dang, Keming Lu, Keqin Chen, Kexin Yang, Mei Li, Mingfeng Xue, Na Ni, Pei Zhang, Peng Wang, Ru Peng, Rui Men, Ruize Gao, Runji Lin, Shijie Wang, Shuai Bai, Sinan Tan, Tianhang Zhu, Tianhao Li, Tianyu Liu, Wenbin Ge, Xiaodong Deng, Xiaohuan Zhou, Xingzhang Ren, Xinyu Zhang, Xipin Wei, Xuancheng Ren, Yang Fan, Yang Yao, Yichang Zhang, Yu Wan, Yunfei Chu, Yeqiong Liu, Zeyu Cui, Zhenru Zhang, and Zhihao

Fan. Qwen2 technical report. *arXiv preprint arXiv:2407.10671*, 2024. [1](#)

- [61] Xiangpeng Yang, Linchao Zhu, Xiaohan Wang, and Yi Yang. Dgl: Dynamic global-local prompt tuning for text-video retrieval. In *Proceedings of the AAAI Conference on Artificial Intelligence*, pages 6540–6548, 2024. [6](#)
- [62] Jiahui Yu, Zirui Wang, Vijay Vasudevan, Legg Yeung, Mojtaba Seyedhosseini, and Yonghui Wu. Coca: Contrastive captioners are image-text foundation models. *Transactions on Machine Learning Research*, 2022. [4](#)
- [63] Jieyu Zhao, Tianlu Wang, Mark Yatskar, Ryan Cotterell, Vicente Ordonez, and Kai-Wei Chang. Gender bias in contextualized word embeddings. In *Conference of the North American Chapter of the Association for Computational Linguistics: Human Language Technologies (NAACL-HLT)*, pages 629–634, 2019. [9](#)
- [64] Shuai Zhao, Linchao Zhu, Xiaohan Wang, and Yi Yang. Centerclip: Token clustering for efficient text-video retrieval. In *ACM SIGIR International Conference on Research and Development in Information Retrieval (SIGIR)*, pages 970–981, 2022. [6](#)